

Perturbative and non-perturbative parts of eigenstates and local spectral density of states: the Wigner band random matrix model

Wen-ge Wang

Department of Physics, South-east University, Nanjing 210096, China

International Center for the Study of Dynamical Systems, University of Milan at Como, via Lucini 3, 22100 Como, Italy

Department of Physics and Centre for Nonlinear Studies, Hong Kong Baptist University, Hong Kong, China

(October 9, 2018)

A generalization of Brillouin-Wigner perturbation theory is applied numerically to the Wigner Band Random Matrix model. The perturbation theory tells that a perturbed energy eigenstate can be divided into a perturbative part and a non-perturbative part with the perturbative part expressed as a perturbation expansion. Numerically it is found that such a division is important in understanding many properties of both eigenstates and the so-called local spectral density of states (LDOS). For the average shape of eigenstates, its central part is found to be composed of its non-perturbative part and a region of its perturbative part, which is close to the non-perturbative part. A relationship between the average shape of eigenstates and that of LDOS can be explained. Numerical results also show that the transition for the average shape of LDOS from the Breit-Wigner form to the semicircle form is related to a qualitative change in some properties of the perturbation expansion of the perturbative parts of eigenstates. The transition for the half-width of the LDOS from quadratic dependence to linear dependence on the perturbation strength is accompanied by a transition of a similar form for the average size of the non-perturbative parts of eigenstates. For both transitions, the same critical perturbation strength λ_b has been found to play important roles. When perturbation strength is larger than λ_b , the average shape of LDOS obeys an approximate scaling law.

PACS number 05.45.+b

I. INTRODUCTION

The average shape of energy eigenfunctions (EFs), which characterizes the spreading of the eigenstates of a perturbed system over the eigenstates of an unperturbed system, is very important in a wide range of physical fields, from nuclear physics and atomic physics to condensed matter physics. For example, in a recent approach for the description of isolated Fermi systems with finite number of particles, a type of “microcanonical” partition function has been introduced and expressed in terms of the average shape of eigenfunctions [1]. However, up to now only some of the general features of the shape have been known clearly. For example, when perturbation is not strong, generally the shape has a Breit-Wigner form (Lorentzian distribution) [2–5], but in a larger range on the interaction strength, without any simple analytical expression known for the shape, only some phenomenological expressions have been suggested [6–11].

Another quantity, the so-called local spectral density of states (LDOS), has also attracted lots of attention recently [6,7,12–16]. This quantity, known in nuclear physics as the “strength function”, gives information about the “decay” of a specific unperturbed state into other states due to interaction. In particular, the width of the LDOS defines the effective “lifetime” of the unperturbed state. For sufficiently weak coupling, the average shape of LDOS is usually close to the Breit-Wigner form with the half-width having a quadratic dependence on

the interaction strength. On the other hand, when interaction is strong, the shape is model dependent and the half-width is linear in the interaction strength.

Numerically it is already known that for Hamiltonian matrices with band structure generally both the average shape of EFs and that of LDOS can be divided into two parts: central parts and tails with exponential (or faster) decay. However, an analytical definition for such a division has not been achieved yet. A possible clue for this problem comes from a generalization of the so-called Brillouin-Wigner perturbation theory [17] introduced in Ref. [18] for studying long tails of EFs, which tells that analytically EFs can be divided into perturbative and non-perturbative parts with perturbative parts being able to be expanded in a perturbation expansion by making use of the corresponding non-perturbative parts. The relationship between central parts and non-perturbative parts of EFs was not studied in Ref. [18], while it is more important.

The purpose of this paper is to study if the above mentioned generalization of Brillouin-Wigner perturbation theory (GBWPT) can provide deeper understanding for properties of EFs and LDOS, especially the relationship between the two divisions mentioned above for EFs. As a first step, here we study the so-called Wigner band random matrix (WBRM) model, which is one of the simplest models for the application of the GBWPT.

The WBRM was first introduced by Wigner 40 years ago [19] for the description of complex quantum sys-

tems as nuclei. It is currently under close investigation [6,12,13,20–25] since it is believed to provide an adequate description also for some other complex systems (atoms, clusters, etc.) and as well as for dynamical conservative systems with few degrees of freedom, which are chaotic in the classical limit. Unlike the standard Band Random Matrices (see, for example, [26,27]), the theory of WBRM is not well developed. Numerically it is known that different averaging procedures for EFs give different results for their average shape. Specifically, when averaging is done with respect to centers of energy shell, for strong interaction central parts of averaged EFs are close to a form predicted for the LDOS by the semicircle law. On the other hand, for the case of averaging with respect to centroids of EFs, central parts of averaged EFs are obviously narrower than the corresponding LDOS when the so-called Wigner parameter is large and an ergodicity parameter is small [13].

Comparatively, more properties are known for the average shape of the LDOS of the WBRM. For the tails, a corrected analytical expression has been derived in Ref. [6] for weak perturbation and numerically found correct for even strong perturbation [6,11,12]. A more general analytical approach for the LDOS of the WBRM is given in Ref. [12], where an expression for the LDOS is given in terms of a function satisfying an integral equation. In sufficiently weak and extremely strong perturbation cases, the expression gives the well known Breit-Wigner form and semicircle law, respectively. For the transition from the Breit-Wigner form to the semicircle form, although the expression also predicts correct results for the LDOS, the physical explanation for it is not so clear yet. Therefore, it is of interest to study if the GBWPT can throw new light on the above mentioned properties of the EFs and the LDOS of the WBRM.

This paper has the following structure. For the sake of completeness, in section II we give a brief presentation of the GBWPT. Some predictions for properties of EFs of the WBRM are also given in the section. Numerical results for the size of non-perturbative parts of EFs are discussed in section III. It is shown that for the average shape of EFs the averaged non-perturbative part is indeed related to the central part. A region predicted in section II, which is between the non-perturbative part and the (exponentially or faster decaying) tails of an EF, is also studied numerically. Section IV is devoted to a discussion for the relation between the average shape of EFs and that of the LDOS. In section V, some properties of the average shape of LDOS, such as the transition from the Breit-Wigner form to the semicircle form and the dependence of its half-width on perturbation strength, are studied numerically and found to be closely related to properties of the average size of the non-perturbative parts of the corresponding EFs. Finally, conclusions are given in section VI.

II. GENERALIZATION OF BRILLOUIN-WIGNER PERTURBATION THEORY

For the sake of completeness, in this section we first give a brief presentation of the above mentioned generalization of Brillouin-Wigner perturbation theory (GBWPT) [18]. Then, we give a brief discussion for some properties of the EFs of the WBRM.

Generally, consider a Hamiltonian of the form

$$H = H^0 + \lambda V \quad (1)$$

where H^0 is an unperturbed Hamiltonian, V is a perturbation and the parameter λ is for adjusting the strength of the perturbation. For the WBRM with dimension N and band width b , the Hamiltonian matrix considered here is chosen of the form

$$H_{ij} = (H^0 + \lambda V)_{ij} = E_i^0 \delta_{ij} + \lambda v_{ij} \quad (2)$$

where

$$E_i^0 = i \quad (i = 1, \dots, N) \quad (3)$$

are eigenenergies of the eigenstates of H^0 labeled by $|i\rangle$. Off-diagonal matrix elements $v_{ij} = v_{ji}$ are random numbers with Gaussian distribution for $1 \leq |i - j| \leq b$ ($\langle v_{ij} \rangle = 0$ and $\langle v_{ij}^2 \rangle = 1$) and are zero otherwise. Here basis states have been chosen as the eigenstates $|i\rangle$ of H^0 in energy order. Eigenstates of H , labeled by $|\alpha\rangle$, are also ordered in energy,

$$H|\alpha\rangle = E_\alpha|\alpha\rangle, \quad E_{\alpha+1} \geq E_\alpha. \quad (4)$$

In order to obtain the GBWPT, let us divide the set of basis states into two parts, $\{|i\rangle, i = p_1, p_1 + 1, \dots, p_2\}$ and $\{|j\rangle, j = 1, \dots, p_1 - 1, p_2 + 1, \dots, N\}$. This also divides the Hilbert space into two sub-spaces, for which the corresponding projection operators are

$$P \equiv \sum_{i=p_1}^{p_2} |i\rangle\langle i| \quad \text{and} \quad Q \equiv 1 - P. \quad (5)$$

Subspaces related to the projection operators P and Q will be called in the following the P and Q subspaces, respectively. For an arbitrary eigenstate $|\alpha\rangle$, which is split into two orthogonal parts $|t\rangle \equiv P|\alpha\rangle$ and $|f\rangle \equiv Q|\alpha\rangle$ by the projection operators P and Q , by making use of the stationary Schrödinger equation, it can be shown that

$$|\alpha\rangle = |t\rangle + \frac{1}{E_\alpha - H^0} Q \lambda V |\alpha\rangle. \quad (6)$$

Introducing an operator T ,

$$T \equiv \frac{1}{E_\alpha - H^0} Q \lambda V, \quad (7)$$

the iterative expansion of Eq. (6) is of the form

$$|\alpha\rangle = |t\rangle + T|t\rangle + T^2|t\rangle + \cdots + T^{n-1}|t\rangle + T^n|\alpha\rangle. \quad (8)$$

Then, one can see that if the projection operators P and Q are such chosen that

$$\lim_{n \rightarrow \infty} \langle \alpha | (T^\dagger)^n T^n | \alpha \rangle = 0, \quad (9)$$

Eq. (8) gives

$$|\alpha\rangle = |t\rangle + T|t\rangle + T^2|t\rangle + \cdots + T^n|t\rangle + \cdots \quad (10)$$

Here the eigenvalue E_α has been treated as a constant. Eq. (10) is a *generalization* of the so-called *Brillouin-Wigner perturbation expansion (GBWPE)* (for BWPE, see, for example, [17,28]).

Equation (9) is the condition for the GBWPE (10) to hold. Generally, if P and Q subspaces are such chosen that $|E_\alpha - E_j^0|$ is large enough compared with $b\lambda V$ for any basis state $|j\rangle$ in the Q subspace, $|T_\alpha^n\rangle$ will vanish when $n \rightarrow \infty$. Therefore, generally there are many choices for the P and Q operators ensuring Eq. (10) to hold. Among them, the projection operator(s) P with the minimum number of basis states and the corresponding operator(s) Q with the maximum number of basis states will be denoted by P_α and Q_α , respectively, and the corresponding $|t\rangle$ and $|f\rangle$ parts of the state $|\alpha\rangle$ will be denoted by $|t_\alpha\rangle \equiv P_\alpha|\alpha\rangle$ and $|f_\alpha\rangle \equiv Q_\alpha|\alpha\rangle$, respectively. The $|t_\alpha\rangle$ part of the state $|\alpha\rangle$ will be called the *non-perturbative* (NPT) part of $|\alpha\rangle$, and the $|f_\alpha\rangle$ part called the *perturbative* (PT) part of $|\alpha\rangle$. Correspondingly, the eigenfunction of the state $|\alpha\rangle$, i.e., its components in the basis states, can also be divided into NPT and PT parts. Eq. (10) tells that $|f_\alpha\rangle$ can be expressed in terms of $|t_\alpha\rangle$, E_α , λV and H^0 . In what follows, generally the GBWPE (10) will be used to discuss the perturbative parts of eigenstates only.

To achieve a more explicit condition for Eq. (9) to hold, let us write T^n in the following form,

$$T^n = \frac{1}{E_\alpha - H^0} \cdot (\lambda U)^{n-1} \cdot Q\lambda V, \quad (11)$$

where

$$U \equiv QV \frac{1}{E_\alpha - H^0} Q \quad (12)$$

is an operator in the Q subspace. Eq. (11) shows that it is the properties of λU that determines if $T^n|\alpha\rangle$ vanishes when n approaches to ∞ . Indeed, writing eigenstates of the operator U in the Q subspace as $|\nu\rangle$,

$$U|\nu\rangle = u_\nu|\nu\rangle, \quad (13)$$

it is easy to see that if all the values of $|\lambda u_\nu|$ are less than 1, then $T^n|\alpha\rangle$ vanishes when n goes to infinity. Therefore, generally the condition for Eq. (10) (also Eq. (9)) to hold

is that the corresponding λU operator in the Q subspace does not have any eigenvector $|\nu\rangle$ with $|\lambda u_\nu| \geq 1$.

As an application of the above results to the WBRM, let us study the component of an eigenstate $|\alpha\rangle$ on a basis state $|j\rangle$ in the Q_α subspace, $C_{\alpha j} \equiv \langle j|\alpha\rangle$, i.e., a component of the perturbative part $|f_\alpha\rangle$. In what follows, for convenience, we use $|j\rangle$ to indicate a basis state in the Q_α subspace, $|i\rangle$ to indicate a basis state in the P_α subspace and $|k\rangle$ for the general case. Suppose j is larger than p_2 for the P_α subspace, specifically, $p_2 + mb < j \leq p_2 + (m+1)b$ with m being an integer greater than or equal to zero. Noticing that a result of the band structure of the Hamiltonian matrix of the WBRM is that $\langle j|(QV)^n|t_\alpha\rangle$ is zero when n is less than $(m+1)$, from Eqs. (10) and (11) we have

$$\begin{aligned} C_{\alpha j} &= \langle j|(T^{m+1} + T^{m+2} + \cdots)|t_\alpha\rangle \\ &= \langle j|\frac{1}{E_\alpha - H^0}(\lambda U)^m(1 + \lambda U + \cdots)Q\lambda V|t_\alpha\rangle. \end{aligned} \quad (14)$$

Since $Q\lambda V|t_\alpha\rangle$ is a vector in the Q_α subspace, it can be expanded in the eigenstates of U ,

$$Q\lambda V|t_\alpha\rangle = \sum_\nu h_\nu|\nu\rangle. \quad (15)$$

A result of this expansion and Eq. (13) is

$$\begin{aligned} &(1 + \lambda U + (\lambda U)^2 + \cdots)Q\lambda V|t_\alpha\rangle \\ &= \sum_\nu h_\nu(1 + \lambda u_\nu + (\lambda u_\nu)^2 + \cdots)|\nu\rangle \\ &= \sum_\nu \frac{h_\nu}{1 - \lambda u_\nu}|\nu\rangle. \end{aligned} \quad (16)$$

Then, substituting Eq. (16) into Eq. (14), one has

$$C_{\alpha j} = \frac{1}{E_\alpha - E_j^0} \sum_\nu \left[\frac{h_\nu}{1 - \lambda u_\nu} \langle j|\nu\rangle \right] (\lambda u_\nu)^m. \quad (17)$$

Since $|\lambda u_\nu| < 1$ for all ν , the behavior of the long tails of the EFs of the WBRM is more or less like exponential decay as discussed in Ref. [6]. In fact, from the viewpoint of the GBWPT, the proof and arguments given in Ref. [6] for behaviors of long tails of the LDOS of the WBRM are still valid when perturbation is strong.

What is of special interest here is the behavior of $C_{\alpha j}$ for j in the regions of $(p_2, p_2 + b]$ and $[p_1 - b, p_1)$, i.e., for j in the regions of size b just beside the non-perturbative part of the eigenstate. For these j , $m = 0$ in Eq. (17) and it is not necessary for $|C_{\alpha j}|$ to decay exponentially. That is to say, the decaying speed of $|C_{\alpha j}|$ for these j should be slower than that for j larger than $p_2 + b$ or less than $p_1 - b$. The two regions of $j \in (p_2, p_2 + b]$ and $j \in [p_1 - b, p_1)$ will be called the *slope* regions of the eigenstate $|\alpha\rangle$ (the reason for such a name will be clear from numerical results in the next section).

According to Eq. (10), the explicit expression for $C_{\alpha j}$ in terms of elements of the Hamiltonian matrix can be written as

$$C_{\alpha j} = \sum_{i=p_1}^{p_2} \left(\frac{\lambda V_{ji}}{E_\alpha - E_j^0} + \sum_{k \in Q} \frac{\lambda V_{jk}}{E_\alpha - E_j^0} \frac{\lambda V_{ki}}{E_\alpha - E_k^0} \right. \\ \left. + \sum_{k,l \in Q} \frac{\lambda V_{jk}}{E_\alpha - E_j^0} \frac{\lambda V_{kl}}{E_\alpha - E_k^0} \frac{\lambda V_{li}}{E_\alpha - E_l^0} \cdots \right) C_{\alpha i} \quad (18)$$

where $C_{\alpha i} = \langle i | t_\alpha \rangle$. This expression can be written in a simpler form by making use of the concept of path, in analogy to that in the Feynman's path integral theory [29], which can be done as follows. For $(q+1)$ basis states $\{|j\rangle, |k_1\rangle, \dots, |k_{q-1}\rangle, |i\rangle\}$ with only $|i\rangle$ in the P_α subspace, we term the sequence $j \rightarrow k_1 \rightarrow \dots \rightarrow k_{q-1} \rightarrow i$ a *path of q paces* from j to i , if $V_{kk'}$ corresponding to each pace is non-zero. Clearly, paths from j to i are determined by the structure of the Hamiltonian matrix in H^0 representation. Attributing a factor $V_{kk'}/(E_\alpha - E_k^0)$ to each pace $k \rightarrow k'$, the contribution of a path s to $C_{\alpha j}$, denoted by $f_{\alpha s}(j \rightarrow i)$, is defined as the product of the factors of all its paces. Then, $C_{\alpha j}$ in Eq. (18) can be rewritten as

$$C_{\alpha j} = \sum_{i=p_1}^{p_2} \sum_s f_{\alpha s}(j \rightarrow i) C_{\alpha i}. \quad (19)$$

An advantage of expressing $C_{\alpha j}$ in terms of contributions of paths is that it makes it easier to understand the important role played by the size of the non-perturbative part of the EF in determining its shape. Such a size for the state $|\alpha\rangle$ will be denoted by N_p , $N_p \equiv p_2 - p_1 + 1$. (N_p is, in fact, a function of α , but, for brevity, the subscript α will be omitted.) Two values of λ are of special interest when λ increases from zero. One is the smallest λ for $N_p = 2$, indicating the beginning of the invalidity of the ordinary Brillouin-Wigner perturbation theory. The other λ is for the case of $N_p = b$. The value of this λ is of interest since topologically the structure of paths for the case of $N_p \geq b$ is different from that for $N_p < b$. For example, when $N_p \geq b$, paths starting from $j < p_1$ can never reach a j' which is greater than p_2 . That is to say, no path can cross the non-perturbative region. On the other hand, when $N_p < b$, paths can cross the non-perturbative region. One can expect that such a difference should have some effects on the shapes of both EFs and LDOS.

III. NUMERICAL STUDY FOR THE PERTURBATIVE AND NON-PERTURBATIVE PARTS OF EIGENFUNCTIONS

In this section we study numerically the division of EFs into perturbative (PT) and non-perturbative (NPT) parts. Both the individual shape and the average shape of EFs will be studied.

The boundary of the NPT part of a state $|\alpha\rangle$, i.e., the values of p_1 and p_2 , are calculated in the following way. For a Hamiltonian matrix as in Eq. (2), we first diagonalize it numerically and get all its EFs. Then, for an eigenstate $|\alpha\rangle$ with energy E_α , we find out all the pairs of p_1 and p_2 for which the value of $\langle \alpha | (T^\dagger)^n T^n | \alpha \rangle$ could become smaller than a small quantity (say, 10^{-6}) when n goes to infinity. Finally, for the pair of (p_1, p_2) thus obtained with the smallest value of $N_p = p_2 - p_1 + 1$ and the pairs of $(p_1 + 1, p_2)$ and $(p_1, p_2 - 1)$, we calculate eigenvalues of the corresponding U operators in Eq. (12) in order to check out if all the $|\lambda u_\nu|$ for the pair of (p_1, p_2) are less than 1 while some of the $|\lambda u_\nu|$ for each of the other two pairs $(p_1 + 1, p_2)$ and $(p_1, p_2 - 1)$ are larger than 1.

The shape of an eigenstate $|\alpha\rangle$ in the unperturbed states can be defined as

$$W_\alpha(E^0) = \sum_k |C_{\alpha k}|^2 \delta(E^0 - E_k^0). \quad (20)$$

In order to obtain the average shape of eigenstates, different individual distributions $W_\alpha(E^0)$ should be first shifted into a common region. For this, we express $W_\alpha(E^0)$ with respect to E_α before averaging. For α from α_1 to α_2 , with $W_\alpha(E^0)$ expressed as $W_\alpha(E^0 - E_\alpha)$, the average shape of the eigenstates, denoted by $W(E_s^0)$, can be calculated. Numerically, $W(E_s^0)$ are thus calculated: For a state $|\alpha\rangle$, some value of E_s^0 and all k satisfying $|E_s^0 - (E_k^0 - E_\alpha)| < \delta E_w/2$, where δE_w is some quantity chosen for dividing E_s^0 into small regions, we calculate the sum of $\sum_k |C_{\alpha k}|^2$, then take the average of the sum over α from α_1 to α_2 . The result thus obtained is the average value of W in the region $(E_s^0 - \delta E_w/2, E_s^0 + \delta E_w/2)$ and is also denoted by $W(E_s^0)$. Similarly, the values of $W(E_s^0 \pm m\delta E_w)$ ($m = 1, 2, \dots$) can also be calculated. The average shape of eigenstates can also be divided into a NPT part and a PT part by the averaged boundary of the NPT parts of the states $|\alpha\rangle$, denoted by $p_1^a \equiv \langle p_1 - E_\alpha \rangle$ and $p_2^a \equiv \langle p_2 - E_\alpha \rangle$. The size of the NPT part of the average shape of eigenstates is $\langle N_p \rangle \equiv \langle p_2 - p_1 + 1 \rangle$. The values of λ for $\langle N_p \rangle$ beginning to be larger than 1 and for $\langle N_p \rangle = b$ will be denoted by λ_f and λ_b , respectively.

Now let us present the numerical results. The first one is for the case of $N = 300, b = 10$ and $\lambda = 0.6$. This is a case for which N_p can be equal to both 1 and 2. The values of $|C_{\alpha k}|^2 = |\langle k | \alpha \rangle|^2$ for four EFs in the middle energy region ($\alpha = 148 - 151$) are given in Fig. 1. The two vertical dashed-dot straight lines for each case indicate the positions of p_1 and p_2 of the NPT part of the eigenstate, i.e., the boundary of the NPT part. Since $E_k^0 = k$, p_1 and p_2 are also the unperturbed eigenenergies of the corresponding basis states $|k = p_1\rangle$ and $|k = p_2\rangle$. For $\alpha = 148$ and 149 , since $p_1 = p_2 = \alpha$ there is only one vertical dashed-dot line in each case. For $\alpha = 150$ and 151 , there are, in fact, two NPT parts

for each case. In Fig. 1 we give one of them for each case only, i.e., $(p_1, p_2) = (149, 150)$ for $\alpha = 150$ (the other one is $(150, 151)$) and $(p_1, p_2) = (151, 152)$ for $\alpha = 151$ (the other one is $(150, 151)$). Numerically we have found that only for small λ is it possible for an eigenstate to have more than one NPT parts. The average shape of EFs for α from 130 to 170 is given in Fig. 2 with the corresponding values of p_1^a and p_2^a indicated by vertical dashed-dot lines. $\delta E_w = 1$ for calculating this $W(E_s^0)$ function.

As mentioned in section II, another perturbation strength of interest is for the case of N_p being able to equal the band width b of the Hamiltonian matrix. An example for this case is $\lambda = 1.4$. For this value of λ , there is only one NPT part for each state $|\alpha\rangle$, e.g., $N_p = 9, 10, 7, 9$ for $\alpha = 148, 149, 150, 151$, respectively. Individual EFs for $\alpha = 148 - 151$ are presented in Fig. 3 with their boundaries of the NPT parts. Although for an individual EF the value of $|C_{\alpha k}|^2$ could be still large outside the NPT region (Fig. 3), the main body of the average shape of EFs lies obviously in the averaged NPT region as shown in Fig. 4(a). For this averaged EF we still have δE_w equal to 1 and α from 130 to 170. An interesting feature of the distribution $\ln W$ in the slope regions $[p_1^a - b, p_1^a]$ and $[p_2^a, p_2^a + b]$ in Fig. 4(b) is that, as predicted in section II, the decaying speed in the two slope regions is obviously slower than that in the long tail regions. From Fig. 4(a) it is quite clear why we call the regions ‘‘slope’’.

In Ref. [13] the average shape of EFs for different values of the Wigner parameter q ,

$$q = \frac{(\rho v)^2}{b}, \quad (21)$$

and an ergodicity parameter ‘‘ λ_e ’’ (denoted by λ in that paper),

$$\lambda_e = \frac{ab^{3/2}}{4\sqrt{2}c\rho v} \quad \text{with } a \approx 1.2, \quad c \approx 0.92, \quad (22)$$

has been studied numerically. Results in that paper show that when q is small and λ_e not small, e.g., $q = 1$ and $\lambda_e = 3.7$, two averaging procedures, namely, averaging with respect to centers of energy shell, which are close to the perturbed eigenenergies, and averaging with respect to centroids of EFs, give similar results for the average shape of EFs; while for large q and small λ_e , e.g., $q = 90$ and $\lambda_e = 0.24$, the two averaging procedures give different results and a so-called localization in energy shell has been found.

What is of interest here is to study the difference between the above two cases of different parameters q and λ_e from the viewpoints of the GBWPT. In Fig. 5, four examples of individual EFs are given for $\lambda = 4.0$, for which $q = 1.6$ and $\lambda_e = 1.82$. When edge effects can be neglected, from the condition for Eq. (9) to hold given in the above section, it can be shown that the eigenenergies

E_α should be close to the centers of the corresponding NPT regions, that is,

$$E_\alpha \approx \frac{p_2 - p_1}{2}. \quad (23)$$

Here by the NPT region of an EF we mean the region of E_k^0 between the boundaries (dashed-dot lines) of the NPT part of the EF as shown in Fig. 5. Then, since as shown in Fig. 5 centroids of the EFs are generally not far from the centers of the NPT regions, they are generally not far from the corresponding eigenenergies. Therefore, in this case the averaging with respect to the centroids of the EFs and the averaging with respect to the eigenenergies do not have much difference, and the average shape of EFs obtained by the two methods should be more or less similar. However, since there are still some differences between the centroids of the EFs and the eigenenergies, results of the two averaging methods can not be quite close to each other. In fact, as shown in Ref. [13], results of the method of averaging with respect to centroids of EFs should be a little narrower than those of the other method.

The average shape of EFs for α from 130 to 170 and $\lambda = 4.0$ is given in Fig. 6 with $\delta E_w = 3.0$. (In this paper numerically we study the averaging with respect to eigenenergies only.) For this averaged EF the slope regions are even clearer. The sizes of the two slope regions in Fig. 6 are larger than b , the predicted one for a single EF, since the values of N_p for the NPT parts of the eigenstates $|\alpha\rangle$ taken for averaging are not the same. In fact, the variance of the N_p for the states is about 1.56.

For studying the case of localization in energy shell as in Ref. [13], the dimension $N = 300$ is too small. Therefore, we increase the value of N to 900 and study the case of $b = 10$ and $\lambda = 30.0$, for which the parameters q and λ_e are equal to 90 and 0.24, respectively, as those in Ref. [13]. The values of $|C_{\alpha k}|^2$ (dots) of four EFs in the middle energy region are given in Fig. 7 with the corresponding boundaries (p_1 and p_2) of the NPT parts of the EFs (indicated by vertical dashed-dot lines). Clearly the main body of each of the EFs occupies only part of the NPT region. Then, resorting to Eq. (23), it is easy to see that for the average shape of EFs the result of averaging with respect to centroids of EFs should be obviously narrower than that of averaging with respect to eigenenergies. This phenomenon is called localization in energy shell in Ref. [13]. In our opinion, it is, in fact, localization of EFs in their NPT regions.

Although, as shown in Fig. 7, when $\lambda = 30.0$ many components of the EFs are quite small in the NPT parts, they can still be distinguished from those in the PT parts. In Fig. 8 we present the values of $|C_{\alpha k}|^2$ in Fig. 7 in logarithm scale, from which the difference between the $|C_{\alpha k}|^2$ in the NPT parts and those in the PT parts is quite clear. In fact, it can be seen from Fig. 8 that $|C_{\alpha k}|^2$

for small components in the NPT parts also decay exponentially on average, but the decaying speed is slower than that for components in the PT parts. Similar results have also been found for other eigenfunctions and the centroids of the EFs have been found scattered in the NPT regions. Therefore, averaging with respect to eigenenergies (around the centers of the NPT regions) is reasonable when studying the average shape of EFs. The average shape of EFs in the middle energy region for α from 420 to 480 is shown in Fig. 9 ($\delta E_w = 10$). The two slope regions are also obvious. The widths of the two slope regions, which can be seen from the figure is about $2\delta E_w = 2b$, are also larger than that predicted for a single EF due to the fact that the variance of N_p for these states $|\alpha\rangle$ is about 5.14.

In order to have a clear picture for the variation of the average size $\langle N_p \rangle$ of NPT parts of EFs with the perturbation strength λ , we plot it in Fig. 10(a) (for $N = 300$ and α from 130 to 170). The two solid straight lines in the figure show that $\langle N_p \rangle$ has a good linear dependence on λ in the two regions of $\lambda \in (2.0, 4.5)$ and $\lambda \in (4.5, 7.0)$. The variation of $\langle N_p \rangle$ for λ less than 2 is given in the inset of the figure in more detail. The solid curve in the inset is a fitting curve of a quadratic form: $(7.5(\lambda - 0.4)^2 + 1.0)$. Since in this case the value of λ_f is a little larger than 0.4, i.e., for $\lambda \leq 0.4$ the size N_p of the NPT parts of the EFs is equal to one, the region of $\lambda < 0.4$ has been neglected when fitting the $\langle N_p \rangle$ by the quadratic curve. From the inset it can be seen that the fitting curve fits the values of $\langle N_p \rangle$ quite well in the region of $\lambda \in (0.4, 1.5)$. Interestingly, the value of λ_b for $\langle N_p \rangle = b$ is between 1.45 and 1.5, that is to say, in the region of $\lambda \in (\lambda_f, \lambda_b)$, the values of $\langle N_p \rangle$ have a quadratic dependence on λ .

The variance of N_p , denoted by ΔN_p , is given in Fig. 10(b) (circles), which shows that ΔN_p is small compared with N_p . From the figure it can be seen that for $\lambda < 5$ the value of ΔN_p increases with λ on average. Then, since, as mentioned above, the value of ΔN_p is about 5.14 when $\lambda = 30$, it does not change much in the region of $\lambda \in (5, 30)$, that is to say, the relative value of the variance, namely $\Delta N_p/N_p$, becomes even smaller as λ becomes larger.

IV. RELATIONSHIP BETWEEN THE SHAPE OF EIGENFUNCTIONS AND OF LDOS

The existence of a relationship between the average shape of EFs and that of LDOS in some particular cases has already been noticed numerically by several authors (see, for example, [13,16,18]). Here for the WBRM we show that some analytical arguments can be given for it by making use of the GBWPT.

The so-called local spectral density of states (LDOS) for an unperturbed state $|k\rangle$ is defined as

$$\rho_L^k(E) = \sum_{\alpha} |C_{\alpha k}|^2 \delta(E - E_{\alpha}) \quad (24)$$

where $C_{\alpha k} = \langle k|\alpha\rangle$. Making use of the division of EFs into NPT and PT parts, the non-perturbative (NPT) and perturbative (PT) part of the LDOS can be defined in the following way. Let us consider all the perturbed states $|\alpha\rangle$ for which $C_{\alpha k}$ is in the NPT parts of their eigenfunctions. Suppose α_{p_1} is the smallest one among these α and α_{p_2} is the largest one among them, i.e., $|\alpha_{p_1}\rangle$ has the smallest eigenenergy and $|\alpha_{p_2}\rangle$ has the largest. A property of the WBRM is that for any state $|\alpha\rangle$ with $\alpha_{p_1} \leq \alpha \leq \alpha_{p_2}$, generally to say, $C_{\alpha k}$ is in the NPT part of its eigenfunction. Then, the non-perturbative (NPT) part of the LDOS $\rho_L^k(E)$ can be defined as the sum in Eq. (24) over $\alpha \in [\alpha_{p_1}, \alpha_{p_2}]$, and the perturbative (PT) part can be defined as the sum over the rest α . The size of the NPT part of the LDOS is defined as $(\alpha_{p_2} - \alpha_{p_1} + 1)$ and will be denoted by N_{α_p} .

The average shape of LDOS, denoted by $\rho_L(E_s)$, can be obtained in a way similar to that for the EFs discussed in section III, except that for the LDOS the distributions $\rho_L^k(E)$ are expressed as functions of $(E - E_k^0)$ before averaging. Since E_k^0 is also the centroid of $\rho_L^k(E)$, such an averaging method is the most natural one. The average shape of LDOS can also be divided into a NPT part and a PT part by the averaged boundary of the NPT parts of the individual LDOS.

Before discussing the relation between the average shape of EFs and that of LDOS, let us first draw some conclusions for properties of EFs from the numerical results discussed in section III. Firstly, based on the numerical results given in section III for the average shape of EFs, we can make such an approximate treatment for the average values of $|C_{\alpha i}|^2$ in the NPT parts of EFs: for a given λ not extremely large, they can be treated as a constant denoted by t_{λ}^2 , i.e., $\overline{|C_{\alpha i}|^2} \approx t_{\lambda}^2$, when edge effects can be neglected. Here we would like to stress that Figs. 2,4,6,8 show that the values of $\overline{|C_{\alpha i}|^2}$ on the edges of the NPT parts become smaller than those in the middle regions when λ increases and the above approximate treatment may fail in case of extremely large λ . Secondly, another result of the last section is that the variance ΔN_p is small compared with N_p . This means that when discussing approximate relations it is reasonable to treat the size N_p of NPT parts of eigenstates as a constant for a fixed λ .

As results of the above two approximations and the approximate relation (23), it can be shown that, under the corresponding conditions, (a) the average value of $|C_{\alpha k}|^2$ in the NPT parts of LDOS is also about t_{λ}^2 , (b) the size of the NPT part of a LDOS is close to that of an EF, i.e., $N_{\alpha_p} \approx N_p$, (c) usually E_k^0 is in the middle region of the NPT part of the LDOS $\rho_L^k(E)$, i.e., $E_k^0 - E_{\alpha_{p_1}} \approx E_{\alpha_{p_2}} - E_k^0$. Then, one can see that the following approximate relation holds for the NPT part

of an averaged EF W and the NPT part of an averaged LDOS ρ_L ,

$$\frac{W(E)}{\rho^0(E)} \approx \frac{\rho_L(E)}{\rho(E)} \quad (25)$$

where $\rho^0(E)$ and $\rho(E)$ are the averaged density of states of the unperturbed and perturbed spectra in the corresponding regions, respectively,. Here, for brevity, instead of E_s^0 and E_s , we use E to denote the variables of the functions W and ρ_L .

Next let us discuss the relation between the PT part of the average shape of EFs and the PT part of the average shape of LDOS. According to Eq. (19), $C_{\alpha j}^2$ for a basis state $|j\rangle$ in the Q_α subspace can be written as

$$C_{\alpha j}^2 = \sum_{i_1=p_1}^{p_2} \sum_{i_2=p_1}^{p_2} \sum_{s_1, s_2} f_{\alpha s_1}(j \rightarrow i_1) f_{\alpha s_2}(j \rightarrow i_2) C_{\alpha i_1} C_{\alpha i_2}. \quad (26)$$

Following a way similar to that of calculating the average shape of EFs $W(E_s)$ in the last section, we take the average of this quantity over different eigenfunctions. Since $C_{\alpha i}$ in the NPT parts of EFs have random signs, the main contribution to $C_{\alpha j}^2$ in Eq. (26) comes from the $i_1 = i_2$ terms and

$$\overline{C_{\alpha j}^2} \approx \sum_{i=p_1}^{p_2} \sum_{s_1, s_2} \overline{f_{\alpha s_1}(j \rightarrow i) f_{\alpha s_2}(j \rightarrow i) t_\lambda^2}. \quad (27)$$

When the number of eigenstates taken for averaging is large enough, since $f_{\alpha s}$ is a product of factors $V_{kk'}/(E_\alpha - E_k^0)$, the main contribution in (27) to $\overline{C_{\alpha j}^2}$ comes from the terms with path s_1 equal to path s_2 , that is,

$$\overline{C_{\alpha j}^2} \approx \sum_{i=p_1}^{p_2} \sum_s \overline{f_{\alpha s}^2(j \rightarrow i) t_\lambda^2}. \quad (28)$$

Let us first discuss the relation (27), which is for cases without enough eigenstates taken for averaging. In these cases, due to the signs of the denominators $(E_\alpha - E_k^0)$ of the factors of paces, there is a systematic difference between the contribution of paths starting from j with $E_j^0 < E_\alpha$ and the contribution of paths starting from j' with $E_{j'}^0 > E_\alpha$, especially when $N_p \geq b$. A result of this difference is that $|C_{\alpha j}|^2$ for the left PT part of an averaged EF may be different from the corresponding one for its right PT part. But, for PT parts of averaged EFs on the same side, such a difference does not exist. In fact, when edge effects can be neglected, the structure of paths is similar for different EFs when the difference in the size of NPT parts of the EFs can be neglected, and we have

$$\overline{f_{\alpha s_1}(j \rightarrow i) f_{\alpha s_2}(j \rightarrow i)} \approx \overline{f_{\alpha' s'_1}(j' \rightarrow i') f_{\alpha' s'_2}(j' \rightarrow i')} \quad (29)$$

where s'_1 s'_2 are paths similar to s_1 and s_2 , respectively, but from j' to i' with $j' - i' = j - i$ and $j' - p'_1 = j - p_1$. From the relations (27) and (29), one can see that, when edge effects can be neglected, the left (right) PT parts of averaged EFs in different energy regions should be similar. By definition, the left (right) PT part of the average shape of EFs should be related to the right (left) PT part of the average shape of LDOS, since, for example, a $|C_{\alpha j}|^2$ in the left PT part of the EF $W_\alpha(E^0)$ is in the right PT part of the LDOS $\rho_L^j(E)$. Then, the relationship between the PT part of the average shape of EFs and that of the average shape of LDOS should be

$$\frac{W(E)}{\rho^0(E)} \approx \frac{\rho_{-L}(E)}{\rho(E)} \quad (30)$$

where $\rho_{-L}(E)$, the inverted LDOS, is defined as $\rho_{-L}(E) \equiv \rho_L(-E)$. This means that the left (right) tail of the average shape of EFs is more similar to the right (left) tail of the average shape of LDOS than its right (left) tail does. Since $|C_{\alpha i}|^2$ can be approximately treated as a constant for the NPT parts of both EFs and LDOS, the approximate relation (30) also holds for the NPT parts of the average shape of EFs and of LDOS.

When there are enough eigenstates taken for averaging, we have the relation (28). In this case, instead of (29), we have

$$\overline{f_{\alpha s}^2(j \rightarrow i)} \approx \overline{f_{\alpha' s'}^2(j' \rightarrow i')}, \quad (31)$$

and the left PT part of an averaged EF should be similar to its right PT part. Then, the same relation as in (25) can be obtained for the PT part of the average shape of EFs and the PT part of the average shape of LDOS. In this case, $\rho_L(E_s) \approx \rho_{-L}(E_s)$.

The above results have been checked by numerical calculations. In Fig. 11(a) and (b), an average shape of EFs $W(E)$ (circles) is compared with a corresponding inverted average shape of LDOS $\rho_{-L}(E)$ (solid curve) for $\lambda = 4.0$ and $b = 10$. In order to avoid edge effects, N is chosen to be 900. In this case, in the middle energy regions the difference between $\rho(E)$ and $\rho^0(E)$ can be neglected. The averaging has been done for 60 perturbed and 60 unperturbed states in the middle energy regions, respectively. For this relatively small number of states taken for averaging, one can expect that the relation (25) is not so good as the (30) in the tail region. Indeed, as shown in Fig. 11(c) the LDOS $\rho_L(E)$ (solid curve) is not so close to the $W(E)$ (circles) as the inverted one $\rho_{-L}(E)$ in Fig. 11(b). In order to show the influence of edge effects on the relation (30), in Fig. 11(d) we give a result obtained when N is equal to 300.

Finally, we would like to stress that although the above arguments leading to the approximate relations (25) and (30) are for not very large λ , numerical results in Ref.

[13] show that central parts of averaged EFs (for averaging with respect to eigenenergies) are still close to those of averaged LDOS when λ is quite large. In fact, for a given λ , the approximation $|C_{\alpha i}|^2 \approx t_\lambda^2$ for NPT parts of EFs, which has been employed in the above arguments, is not necessary for deducing the relations (25) and (30). For example, under the approximation that $|C_{\alpha i_1}|^2 \approx |C_{\alpha i_2}|^2$ with $i_1 - p_1 = p_2 - i_2$ for NPT parts of EFs, similar arguments as given above also lead to the two relations (25) and (30). In fact, this approximation is in even better agreement with the numerical results given in the last section than the former approximation $|C_{\alpha i}|^2 \approx t_\lambda^2$ and may be still valid for very large λ . Therefore, the two relations (25) and (30) may be correct for very large λ , too.

V. VARIATION OF THE SHAPE OF LDOS WITH PERTURBATION STRENGTH

Analytical and numerical study for the shape of the LDOS of the WBRM has been done in, e.g., [19,6,12,11]. It is known that when perturbation is weak (but not very weak) the average shape of LDOS is of the Breit-Wigner form (Lorentzian distribution), and when perturbation becomes strong the shape will approach to a form predicted by the semi-circle law.

Our interest here is in studying the process of the transition from the Breit-Wigner form to the semi-circle form, in order to see if the GBWPT can throw light on how the transition occurs. In fact, due to two results of the previous two sections that (a) the central part of the average shape of EFs is composed of its NPT part and the slope region of the PT part and (b) the average shape of EFs is similar to that of LDOS when the density of states of the perturbed spectrum is similar to that of the unperturbed spectrum, one can expect that properties of the average shape of LDOS, particularly of its half-width, should be related to properties of $\langle N_p \rangle$, the average size of NPT parts of EFs.

An interesting property of the semicircle law

$$\rho_{sc}(E) = \frac{2}{\pi R_0^2} \sqrt{R_0^2 - E^2}, \quad |E| \leq R_0, \quad (32)$$

where $R_0 = \lambda\sqrt{8b}$, is that it obeys a scaling law. Specifically, after a rescaling

$$R_0 = \lambda R'_0, \quad E = \lambda E', \quad \rho_{sc}(E) = \rho'_{sc}(E')/\lambda, \quad (33)$$

it becomes

$$\rho'_{sc}(E') = \frac{2}{\pi R_0'^2} \sqrt{R_0'^2 - E'^2}, \quad (34)$$

having the same form as the ρ_{sc} in Eq. (32). In fact, Eq. (34) is just Eq. (32) for the case of $\lambda = 1$. This property of the semicircle law supplies a convenient method of

studying the approaching of the average shape of LDOS $\rho_L(E_s)$ (for brevity, as in the last section, the subscript s for the variable E_s will be omitted in what follows) to the semicircle form $\rho_{sc}(E)$ with increasing λ . That is, first we change the LDOS $\rho_L(E)$ for a perturbation strength λ to a rescaled one $\rho_L^{rs}(E)$ defined by

$$\rho_L^{rs}(E) = \lambda \rho_L(\lambda E), \quad (35)$$

then, we compare it with the semicircle form $\rho_{sc}(E)$ for $\lambda = 1$.

In Fig. 12 we present such comparisons for λ from 1.2 to 1.9. The LDOS $\rho_L(E)$ in this and the following figures are for $N = 500$ and $b = 10$. In order to take average, 30 Hamiltonian matrices of different realizations of the random numbers have been diagonalized for each λ and 50 individual LDOS $\rho_L^k(E)$ in the middle energy region have been taken for each Hamiltonian matrix. Figure 12 shows that the sign for the $\rho_L^{rs}(E)$ to approach the semicircle form appears when λ is between 1.5 and 1.6. Interestingly, in this case the value of λ_b for $\langle N_p \rangle = b$ is also between 1.5 and 1.6. As indicated in section II, such a value of λ is of interest, since for a perturbed eigenstate with $N_p \geq b$ paths starting from the left PT part of the state can not reach the right PT part, and vice versa. That is to say, when λ becomes larger than λ_b , there will be a change in the topological structure of the paths. Therefore, such a coincidence should not be an accident.

When λ becomes larger, as is known, the form of $\rho_L^{rs}(E)$ will become closer to the semicircle form (Fig. 13). Since the semicircle law has a scaling behavior, an interesting result of the comparisons between the rescaled LDOS $\rho_L^{rs}(E)$ and the semicircle form given in Figs. 12 and 13 is that the LDOS $\rho_L(E)$ obeys an approximate scaling law when λ is larger than λ_b . As a consequence, the dependence of the half-width of the LDOS on λ should become linear when λ exceeds λ_b .

The Breit-Wigner form

$$\rho_{BW}(E) = \frac{\Gamma/2\pi}{E^2 + \Gamma^2/4} \quad (36)$$

does not have the scaling property as the semicircle law. For the purpose of studying the relationship between the Breit-Wigner form and the average shape of LDOS, we use the former as a fitting curve for the later with the width Γ as the fitting parameter. The fitting is done by requiring the minimum of the area difference

$$\Delta S = \int |\rho_L(E) - \rho_{BW}(E)| dE \quad (37)$$

between the Breit-Wigner form and the histogram of the averaged LDOS. In numerical calculations, we first change the Breit-Wigner form to a histogram corresponding to the histogram of the LDOS, then calculate the ΔS .

Four examples thus obtained for $\lambda = 0.4, 0.7, 1.0$ and 1.5 are given in Figs. 14 and 15. From numerical results we have found that the average shape of LDOS begins to be fitted well by the Breit-Wigner form just before λ reaches 0.4. Interestingly, the value of λ_f for $\langle N_p \rangle$ beginning to be larger than 1 is a little larger than 0.4. That is to say, the LDOS of the Breit-Wigner form begins to appear just before the ordinary Brillouin-Wigner perturbation theory fails. With the increasing of λ , the closeness between the LDOS and the Breit-Wigner form maintains for a small region of the λ . Then, when λ increases further, deviation will become more obvious. In fact, when $\lambda = \lambda_b \approx 1.5$, the LDOS $\rho_L(E)$ is absolutely different from the Breit-Wigner form, while it becomes closer to the semicircle form.

Since the smallest area difference ΔS in Eq. (37) gives a measure for the deviation of the average shape of LDOS from the Breit-Wigner form, we plot it in Fig. 16 (squares). It can be seen that the deviation reaches its saturated value at about $\lambda = 2.0$. Similarly, in order to show the deviation of the average shape of LDOS from the semicircle form, one can introduce another area difference

$$\Delta S = \int |\rho_L^{rs}(E) - \rho_{sc}(E)| dE \quad (38)$$

where $\rho_{sc}(E)$ is for $\lambda = 1$. Variation of this ΔS with λ is also given in Fig. 16 (circles). It shows that before λ reaches 1.5 the deviation is large and drops quickly. For λ from 1.5 to about 4.5, ΔS drops slower. When λ is larger than 4.5, the values of ΔS are quite small and change quite slowly, which means that the average shape of LDOS has become quite close to the semicircle form.

Variation of the half-width of the average shape of LDOS is of both experimental and theoretical interest. Such a variation is given in Fig. 17 by triangles. As expected, when λ exceeds $\lambda_b \approx 1.5$, the half-width can be fitted well by a straight line. The variation of $\langle N_p \rangle$ with λ is also given in Fig. 17 (circles). Corresponding to the three regions of λ for the variation of the ΔS measuring the deviation of the LDOS from the semicircle form represented by circles in Fig. 16, the variation of $\langle N_p \rangle$ can also be divided into three regions: (1) $\lambda < 1.5$, (2) $1.5 < \lambda < 4.5$, in which it can be fitted well by a straight line, and (3) $\lambda > 4.5$, in which it can be fitted well by another straight line.

The fitting for the half-width of the LDOS and for the $\langle N_p \rangle$ for small λ is given in the upper-left inset in Fig. 17. Since when $\lambda < 0.4$ the value of $\langle N_p \rangle$ equals to 1, the fitting for $\langle N_p \rangle$ (circles) has been done for $\lambda > 0.4$ by a quadratic curve $(a(\lambda - 0.4)^2 - 1.0)$ with $a \approx 7.0$. The quadratic feature of the dependence of $\langle N_p \rangle$ on λ is quite clear in the region of $0.4 < \lambda < 1.5$. For the half-width (triangles), the same form of fitting curve with $a \approx 15.0$ is also given in the inset. As expected, the quadratic feature is also clear for the half-width in the region of

$0.4 < \lambda < 1.5$. Therefore, the correspondence between behaviors of the average size of NPT parts of EFs and those of the half width of the average shape of LDOS is quite clear. The lower-right inset in Fig. 17 gives a comparison between the $\langle N_p \rangle$ for $N = 500$ (solid curve) here and the $\langle N_p \rangle$ for $N = 300$ (dashed line) in Fig. 10. The small deviation between them comes from both edge effects and the fact that they are for Hamiltonian matrices with different values of off-diagonal elements.

In conclusion, as expected, numerical results given in this section show that properties of the average shape of LDOS are indeed related to properties of the average size of NPT parts of perturbed eigenstates and knowledge of the latter, especially the value of λ_b for $\langle N_p \rangle = b$, can indeed give deeper understanding for the former.

VI. CONCLUSIONS

The Wigner Band Random Matrix (WBRM) model is studied numerically in this paper by making use of a generalization of the Brillouin-Wigner perturbation theory (GBWPT). According to the GBWPT, an energy eigenfunction (EF) of a perturbed system can be divided into a non-perturbative (NPT) and a perturbative (PT) part with the PT part expressed as a perturbation expansion. Further more, the PT part can be divided into a slope region and a tail region.

Numerically we have found that for the average shape of EFs its central part is composed of its NPT part and the slope region of its PT part. That is, the GBWPT can give an analytical definition for the division of the average shape of EFs into central parts and tails. For the shape of individual EFs, numerical results show that when the perturbation is not strong their NPT part and the slope region of their PT part are usually composed of large components. But when the perturbation becomes stronger, the region of the NPT part of an EF occupied by large components will become relatively smaller, i.e., the ratio of the region to the whole NPT part will become smaller. As for the small components in the NPT part of an EF in this case, the difference between them and the components in the PT part is also obvious. Here we would like to point out that the possibility of dividing EFs into NPT and PT parts should be useful in reducing calculation time for eigenfunctions in a given energy region.

It is already known from some previous numerical studies that there is a relationship between the average shape of EFs and that of LDOS, but the reason is not clear. Resorting to the GBWPT and some conjectures made from numerical results, it is possible to show that such a relationship indeed exist for the WBRM. Particularly, when the number of states taken for averaging is not large enough, the relationship is between the average shape of EFs and the average shape of inverted LDOS.

A result of the above properties of the average shape of EFs and of LDOS is that some properties of the average shape of LDOS should be related to properties of the NPT part of the average shape of EFs. This has been studied in detail by numerical calculations. Firstly, it is found that the LDOS of the Breit-Wigner form appears just before the perturbation strength λ reaches a value λ_f , for which the NPT parts of EFs begin to have more than one components. Secondly, when λ reaches λ_b , for which the average size $\langle N_p \rangle$ of NPT parts of EFs is equal to the band width b of the Hamiltonian matrix, the average shape of LDOS begins to be close to the semicircle form predicted by the semicircle law, and for λ larger than λ_b the average shape of LDOS obeys an approximate scaling law. Thirdly, variation of the half-width of the average shape of LDOS with perturbation strength is closely related to the variation of the average size $\langle N_p \rangle$ of NPT parts of EFs. Particularly, when $\lambda < \lambda_b$, i.e., $\langle N_p \rangle < b$, both of them are of quadratic form, and when λ is larger than λ_b , both of them becomes linear.

Acknowledgements

We are very grateful to G.Casati and F.M.Izrailev for valuable discussions. This work was partly supported by the National Basic Research Project "Nonlinear Science", China, Natural Science Foundation of China, grants from the Hong Kong Research Grant Council (RGC) and the Hong Kong Baptist University Faculty Research Grant (FRG).

[1] V.V. Flambaum and F.M. Izrailev, Phys. Rev. E **56**, 5144 (1997).
[2] B. Georgeot and D.L. Shepelyansky, Phys. Rev. Lett., **79**, 4365 (1997).
[3] Ph. Jacquod and D.L. Shepelyansky, Phys. Rev. Lett., **75**, 3501 (1995).
[4] Y.V. Fyodorov and A.D. Mirlin, Phys. Rev. B **52**, R11580 (1995).
[5] K. Frahm and A. Müller-Groeling, Europhys. Lett. **32**, 385 (1995).
[6] V.V. Flambaum, A.A. Gribakina, G.F. Gribakin, and M.G. Kozlov, Phys. Rev. A **50**, 267 (1994).
[7] V.Zelevinsky, B.A. Brown, M. Horoi and N. Frazier, Phys. Rep., **276**, 85 (1996).
[8] V.V. Flambaum, G.F. Gribakin and F.M. Izrailev, Phys. Rev. E **53**, 5729 (1996).
[9] V.V. Flambaum, F.M. Izrailev and G. Casati, Phys. Rev. E **54**, 2136 (1996).
[10] V.V. Flambaum and F.M. Izrailev, Phys. Rev. E **55**, R13, (1997).
[11] G. Casati, V.V. Flambaum and F.M. Izrailev, (to be published).

[12] Y.V. Fyodorov, O.A. Chubykalo, F.M. Izrailev and G. Casati, Phys. Rev. Lett., **76**, 1603 (1996).
[13] G. Casati, B.V. Chirikov, I. Guarneri and F.M. Izrailev, Phys. Lett. A **223**, 430 (1996).
[14] Ph. Jacquod, D.L. Shepelyansky and O.P. Sushkov, Phys. Rev. Lett. **78**, 923 (1997).
[15] A.D.Mirlin and Y.V.Fyodorov, cond-mat/97002120.
[16] F. Borgonovi, I. Guarneri, F.M. Izrailev and G. Casati, e-print chao-dyn/9711005.
[17] J. M. Ziman, Elements of Advanced Quantum Theory (Cambridge University Press, Cambridge, 1969), p53.
[18] Wen-ge Wang, F. M. Izrailev, and G. Casati, Phys. Rev. E **57**, 323 (1998).
[19] E. Wigner, Ann. Math., **62**, 548 (1955); **65**, 203 (1957).
[20] M. Feingold, D.M. Leitner and O.Piro, Phys. Rev. A **39**, 6507 (1989).
[21] M. Feingold, D. Leitner and M. Wilkinson, Phys. Rev. Lett., **66**, 986 (1991); J. Phys. A **24**, 1751 (1991).
[22] D.M. Leitner and M. Feingold J. Phys. A **26**, 7367 (1993).
[23] G. Casati, B.V. Chirikov, I. Guarneri and F.M. Izrailev, Phys. Rev. E **48**, R1613 (1993).
[24] A. Gioietta, M. Feingold, F.M. Izrailev and L. Molinari, Phys. Rev. Lett. **70**, 2936 (1993).
[25] T. Prosen and M. Robnik, J. Phys. A **26**, 1105 (1993).
[26] Y. V. Fyodorov and A. D. Mirlin, Int. J. Mod. Phys. B **8**, 3795 (1994).
[27] F. M. Izrailev, Chaos, Solitons & Fractals **5**, 1219 (1995).
[28] Xu Gong-ou, Wang Wen-ge and Yang Ya-tian, Phys. Rev. A **45**, 5401 (1992).
[29] R.P. Feynman and R.G. Hibbs, Quantum mechanics and path integrals (McGraw-Hill, New York, 1965).

FIG. 1. Circles show the values of $|C_{\alpha k}|^2 = |\langle k|\alpha \rangle|^2$ for four energy eigenstates $|\alpha \rangle$ when $\lambda = 0.6$ and $N = 300$. The vertical dashed-dot lines indicate the boundaries p_1 and p_2 of the corresponding four non-perturbative parts of the eigenstates (for $\alpha = 148$ and 149 , $p_1 = p_2 = \alpha$).

FIG. 2. (a) The average shape of eigenstates in the middle energy region, $W(E_s)$ (circles), for $\lambda = 0.6$ and $N = 300$. The vertical dashed-dot lines indicate the averaged boundary p_1^a and p_2^a of the corresponding non-perturbative parts of the eigenstates. (b) Same as in (a) in logarithm scale.

FIG. 3. Same as in Fig. 1 for $\lambda = 1.4$.

FIG. 4. Same as in Fig. 2 for $\lambda = 1.4$.

FIG. 5. Same as in Fig. 1 for $\lambda = 4.0$.

FIG. 6. Same as in Fig. 2 for $\lambda = 4.0$.

FIG. 7. Same as in Fig. 1 for $\lambda = 30.0$ and $N = 900$.

FIG. 8. Same as in Fig. 7 in logarithm scale.

FIG. 9. Same as in Fig. 2 for $\lambda = 30.0$ and $N = 900$.

FIG. 10. (a) Variation of the average size $\langle N_p \rangle$ (circles) of non-perturbative parts of eigenstates in the middle energy region with the perturbation strength λ for $N = 300$. The two solid straight lines are fitting lines. The inset shows the fitting curve of the form $7.5(\lambda - 0.4)^2 + 1.0$ for λ from 0.4 to 1.5. (b) Variation of the variance of N_p , ΔN_p (circles), with λ .

FIG. 11. (a) A comparison between an average shape of eigenfunctions $W(E)$ (circles) and a related average shape of inverted LDOS $\rho_{-L}(E)$ (solid curve) for $\lambda = 4.0$ and $N = 900$. (b) Same as in (a) in logarithm scale. (c) A comparison between the $W(E)$ (circles) in (a) and the LDOS $\rho_L(E)$ (solid curve) related to the $\rho_{-L}(E)$ in (a) in logarithm scale. (d) Same as in (b) for $N = 300$.

FIG. 12. Comparisons between the rescaled LDOS ρ_L^{rs} (histograms) obtained when $N = 500$ and the prediction of semicircle law (solid curve) for $\lambda = 1$.

FIG. 13. Same as in Fig. 12 for larger values of λ .

FIG. 14. The average shape of LDOS $\rho_L(E)$ (histograms) obtained when $N = 500$ and the fitting curves (dashed curves) of the Breit-Wigner form.

FIG. 15. Same as in Fig. 14 for larger values of λ .

FIG. 16. Variation of the area difference ΔS (circles) between the rescaled LDOS and the semicircle form for $\lambda = 1$, and variation of the area difference ΔS (squares) between the average shape of LDOS and the fitting Breit-Wigner curves with λ for $N = 500$.

FIG. 17. The triangles show the values of the half-width of the average shape of LDOS, and the circles show the values of the average size $\langle N_p \rangle$ of non-perturbative parts of eigenfunctions when $N = 500$. The three solid straight lines are fitting lines. The upper-left inset shows the fitting curve of the form $(7(\lambda - 0.4)^2 + 1.0)$ for $\langle N_p \rangle$ and the fitting curve of the form $(15(\lambda - 0.4)^2 + 1.0)$ for the half-width of the LDOS for λ from 0.4 to 1.5. The lower-right inset gives a comparison between the $\langle N_p \rangle$ in Fig. 10 obtained when $N = 300$ (dashed curve) and the $\langle N_p \rangle$ here obtained when $N = 500$ (solid curve).

Fig.1

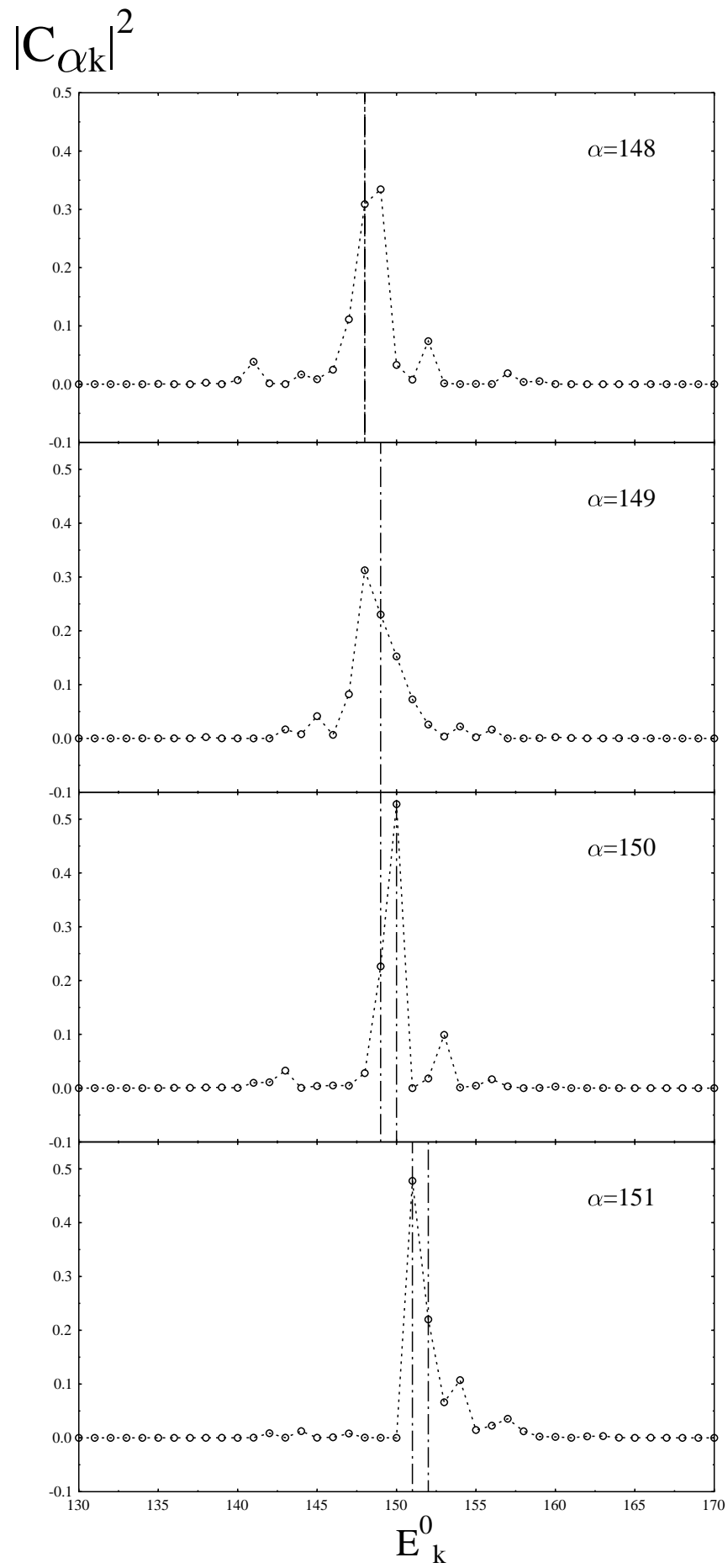
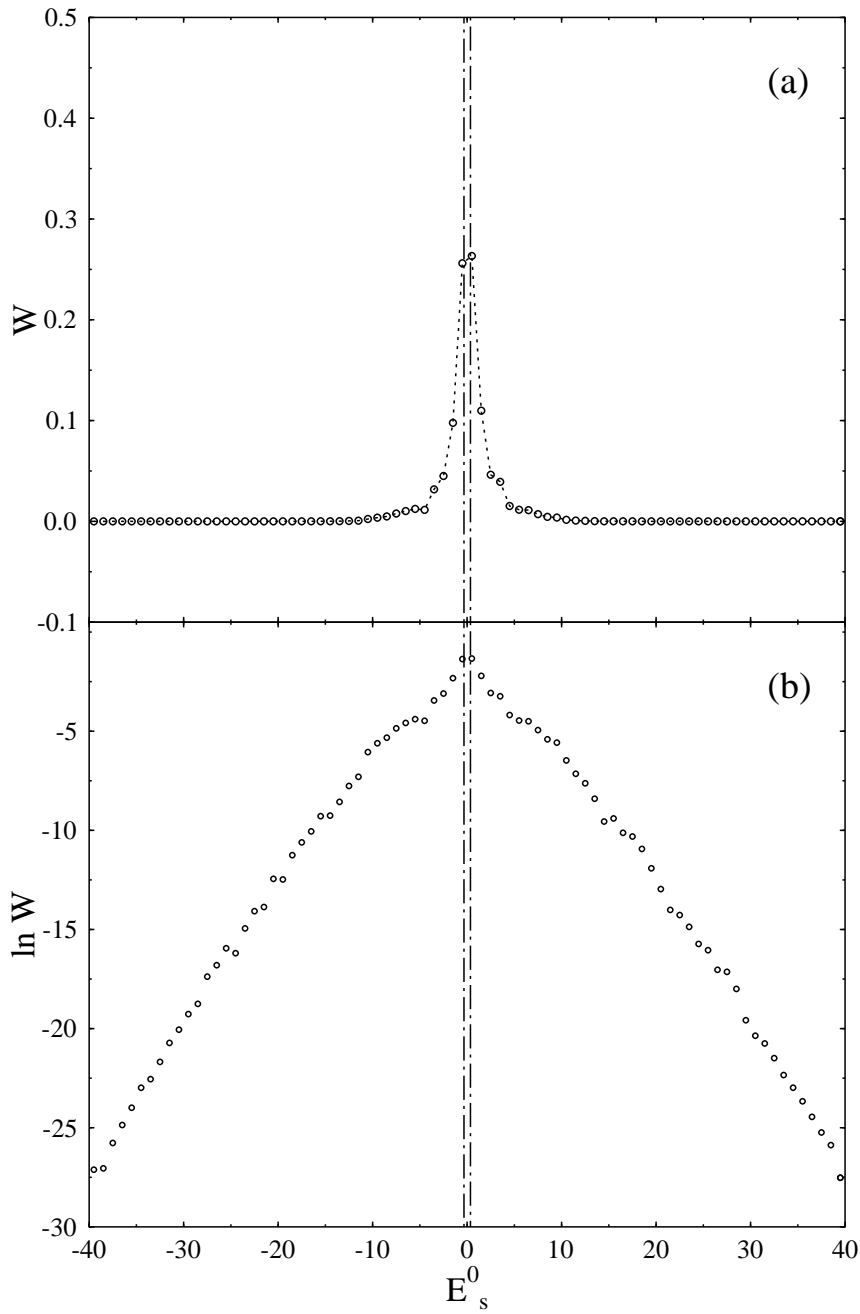


Fig.2



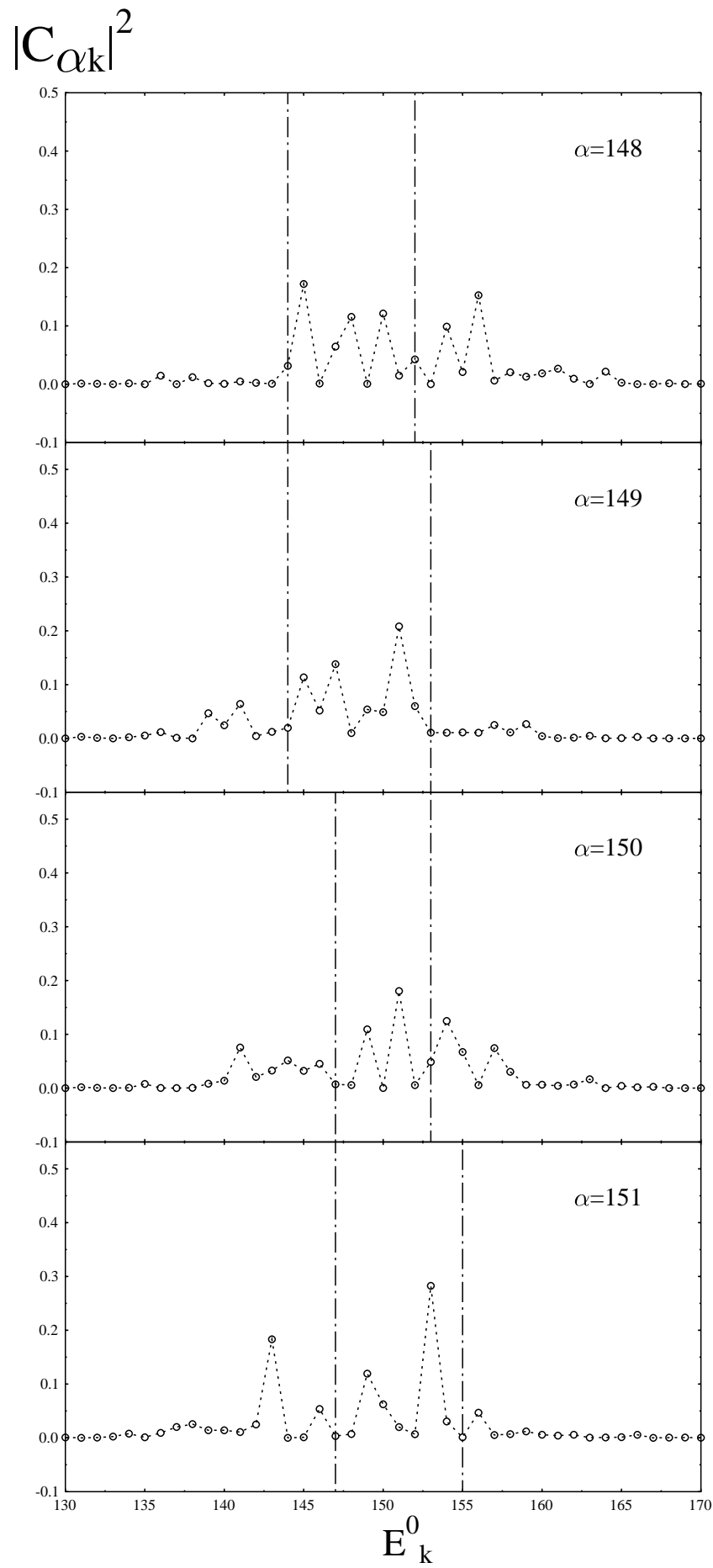


Fig.4

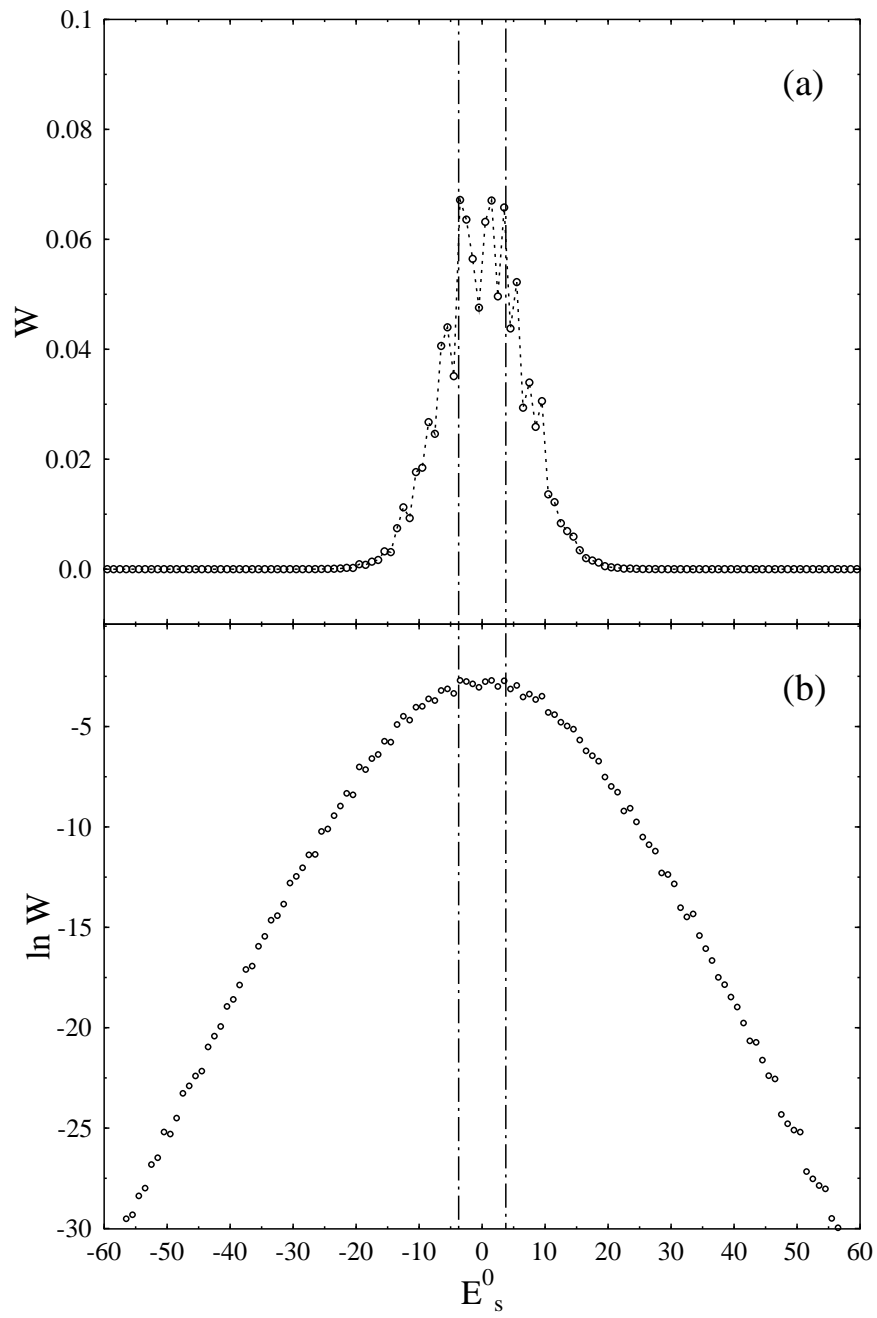


Fig.5

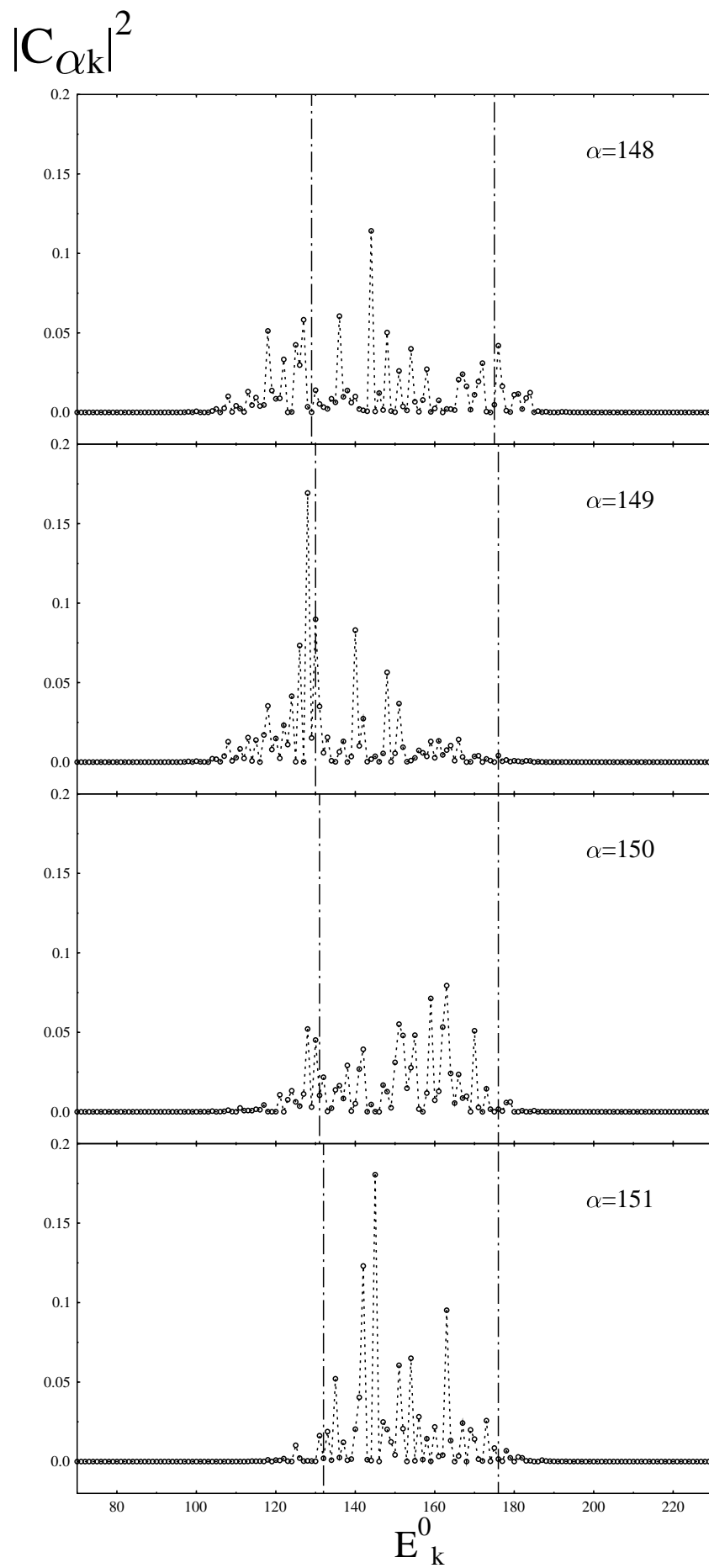
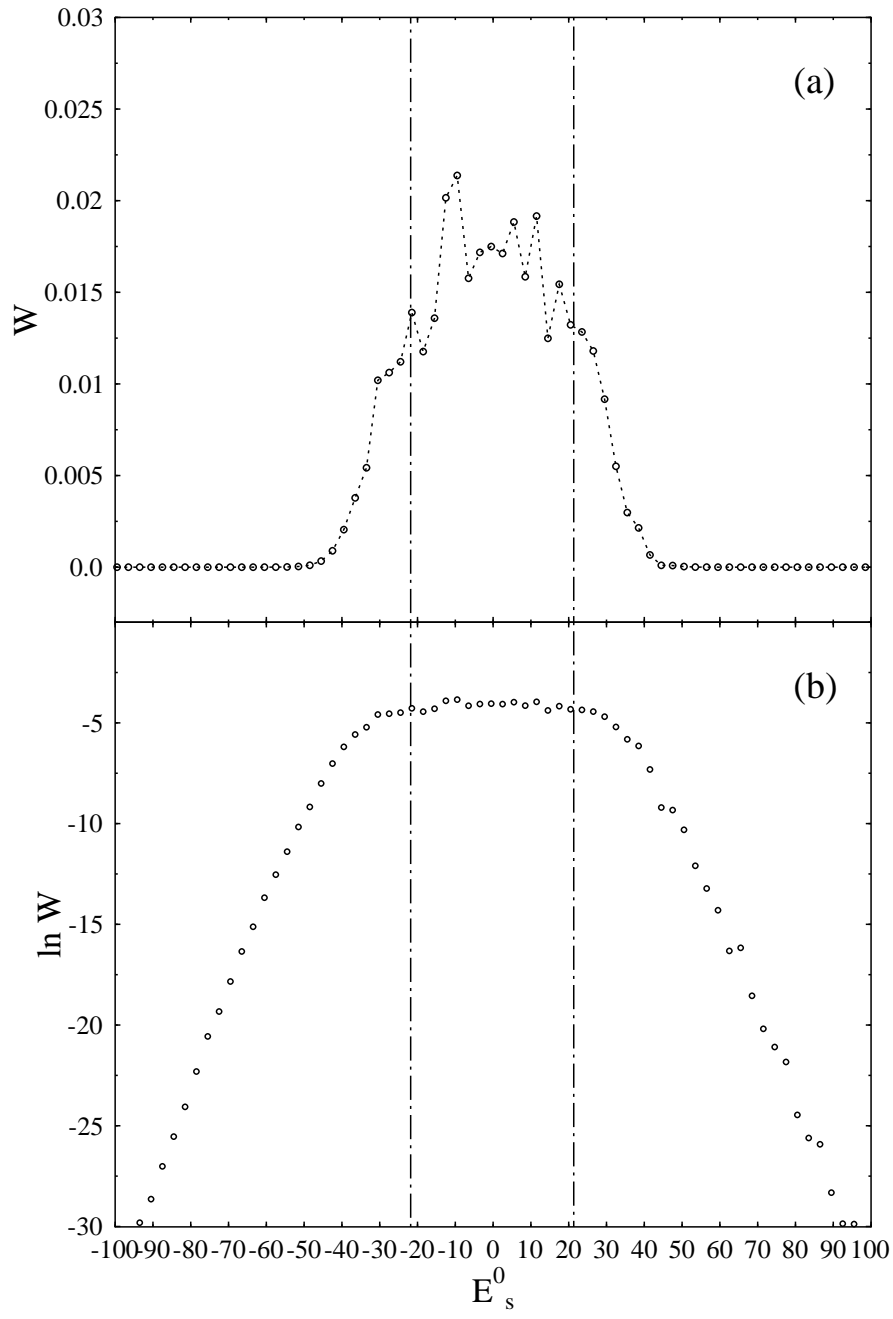
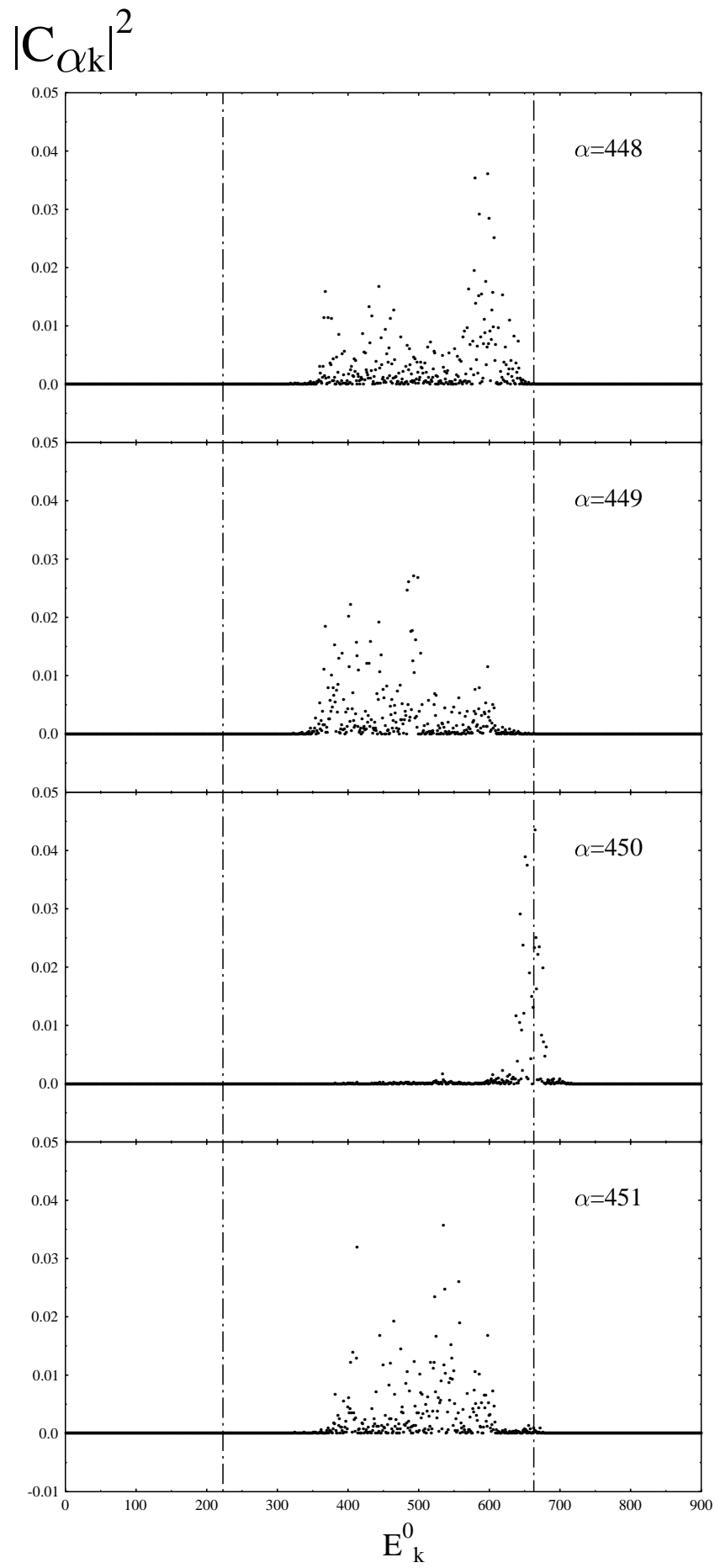


Fig.6





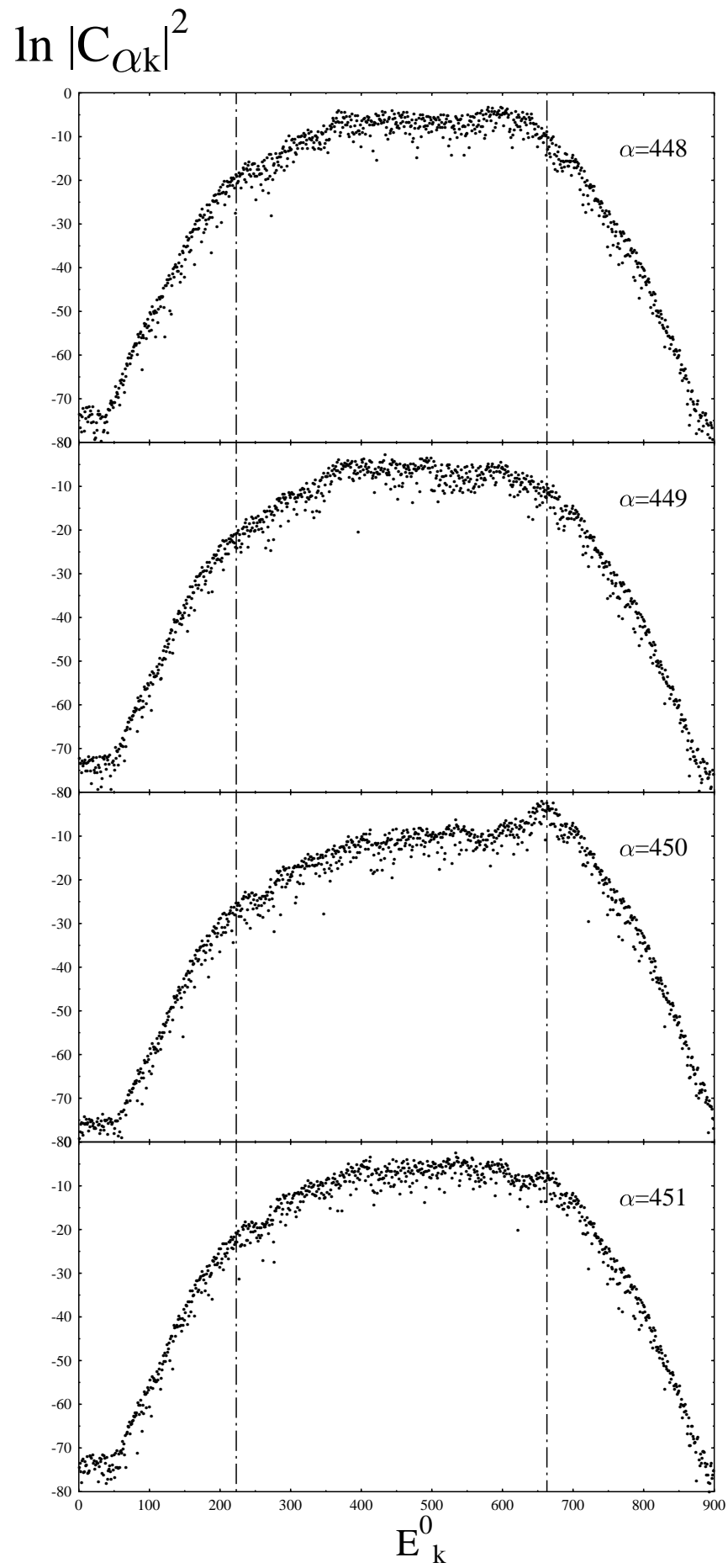


Fig.9

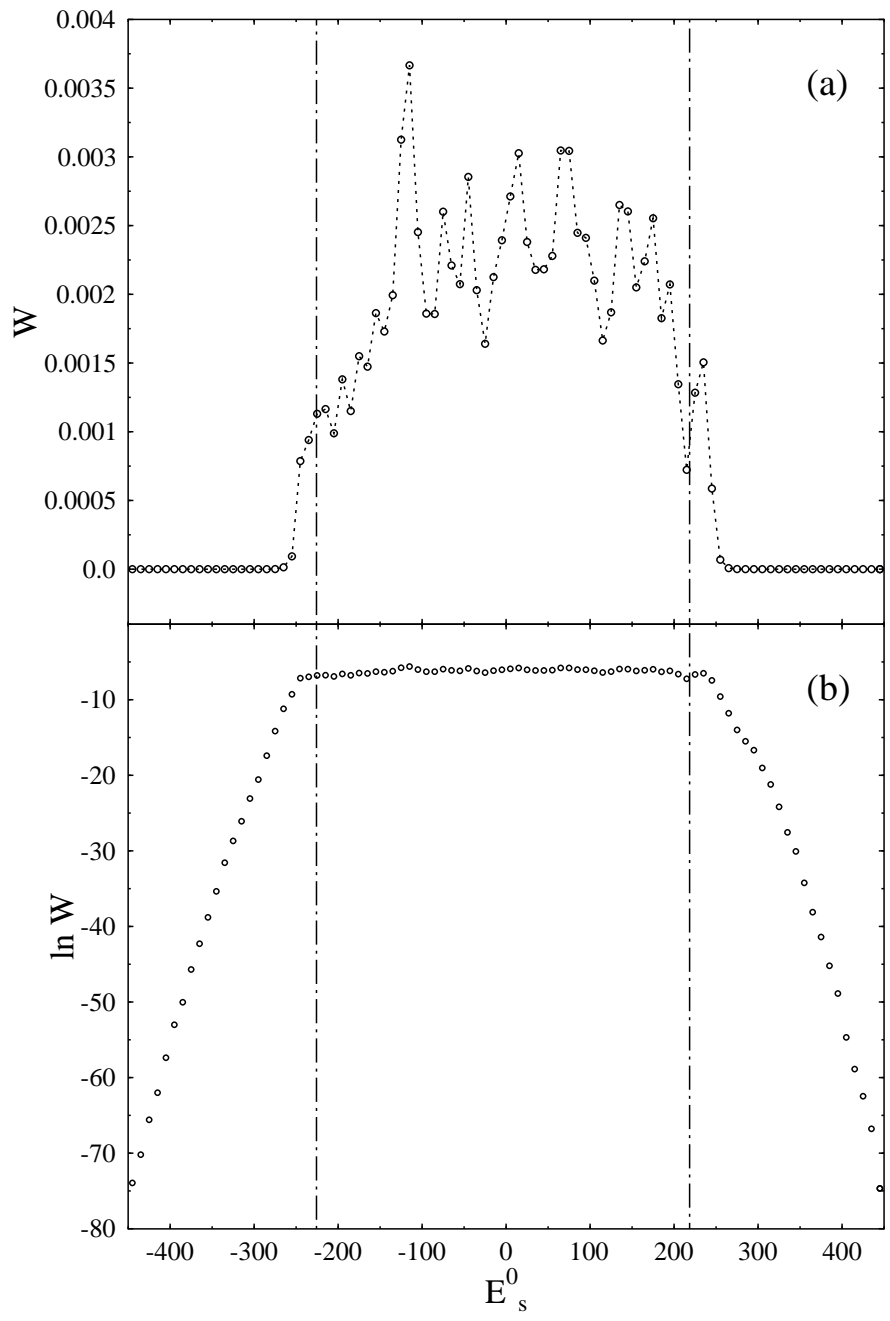


Fig.10

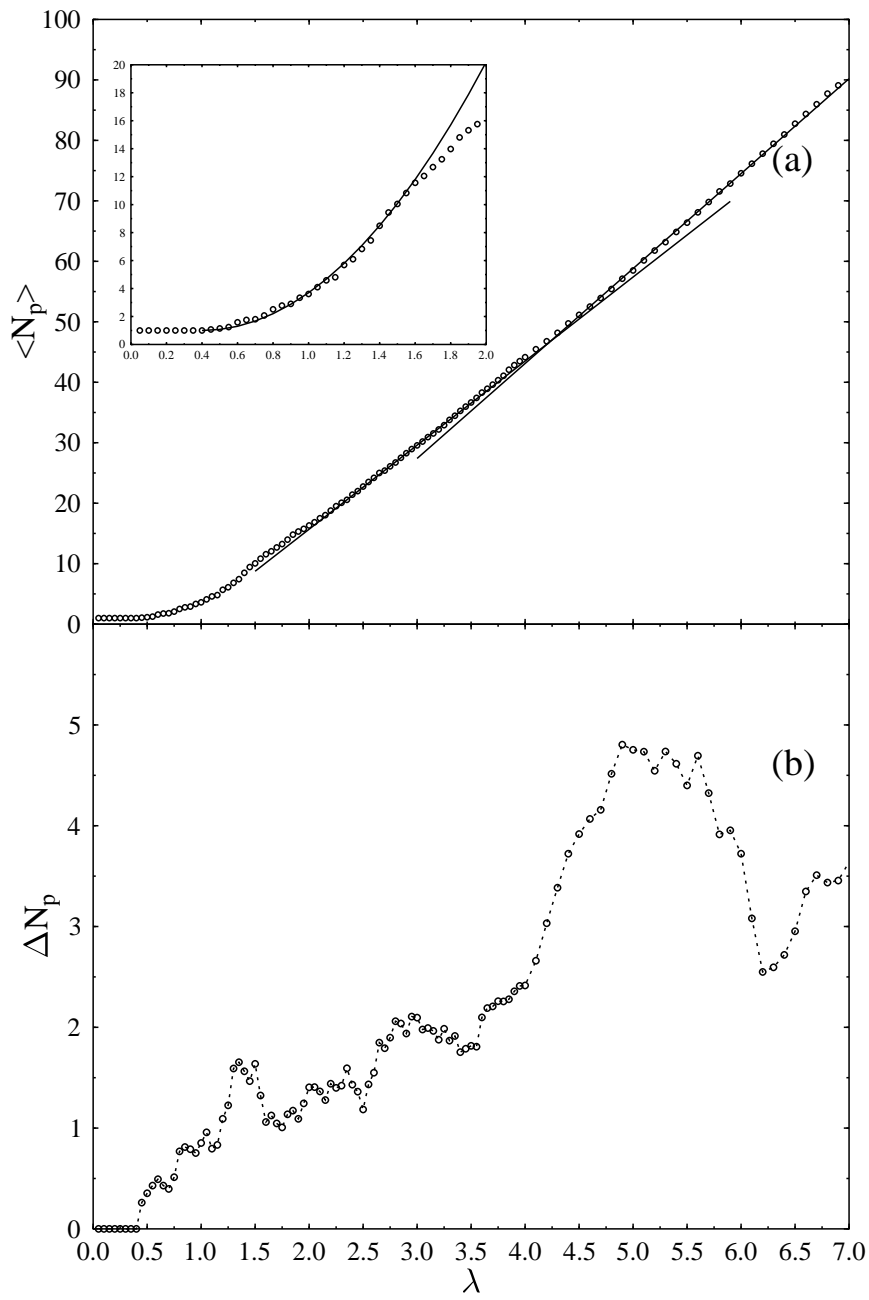
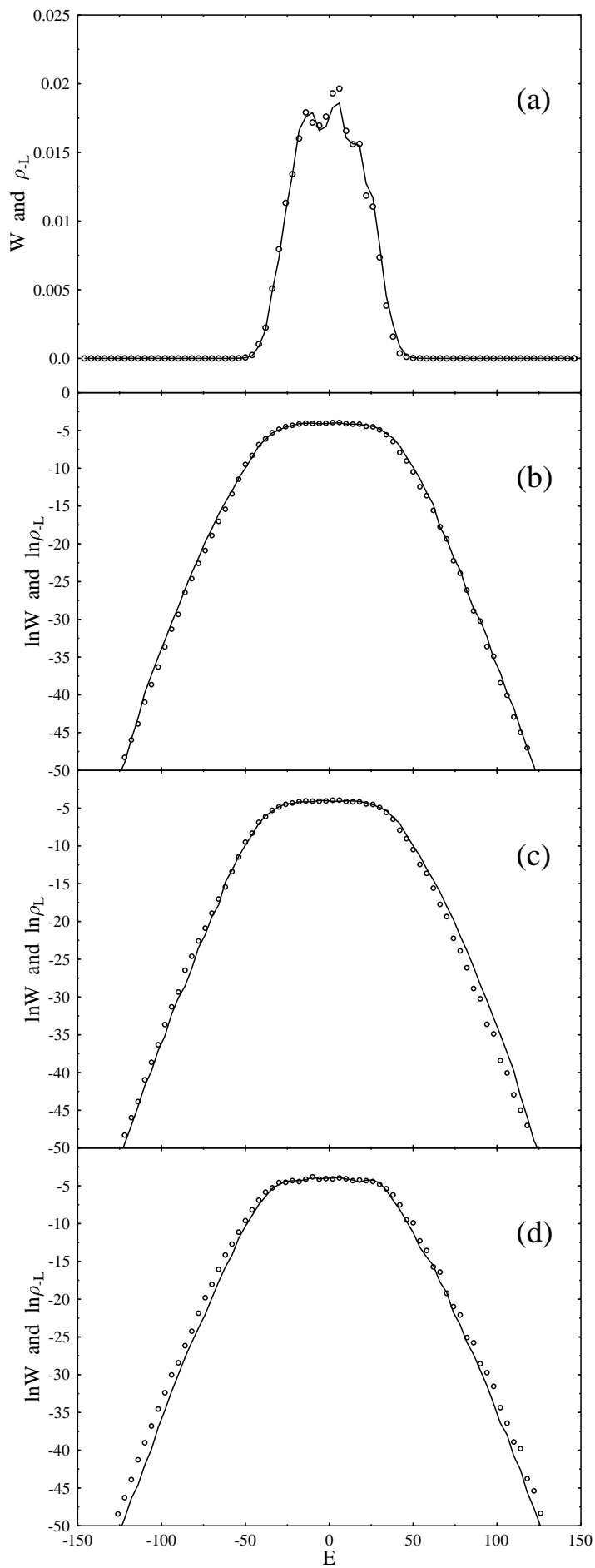
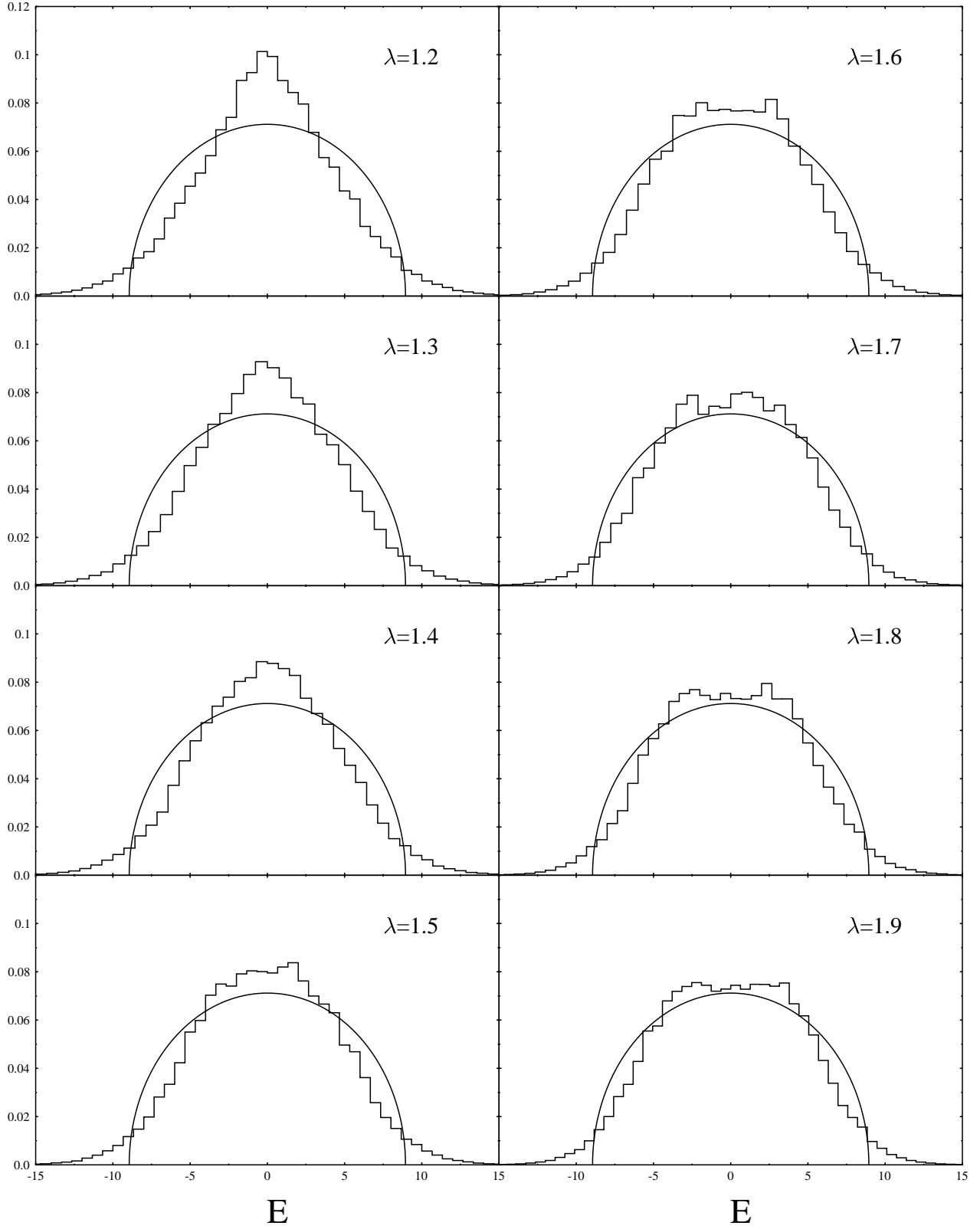
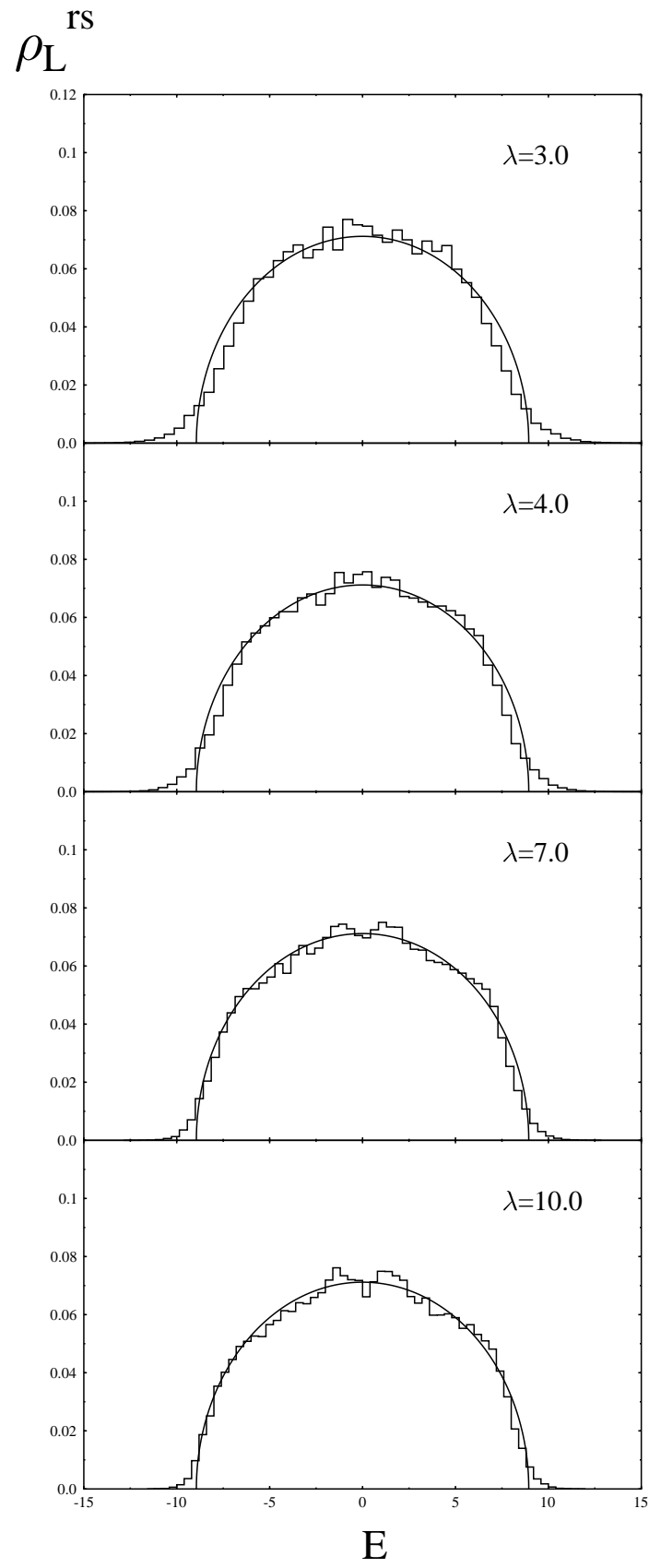
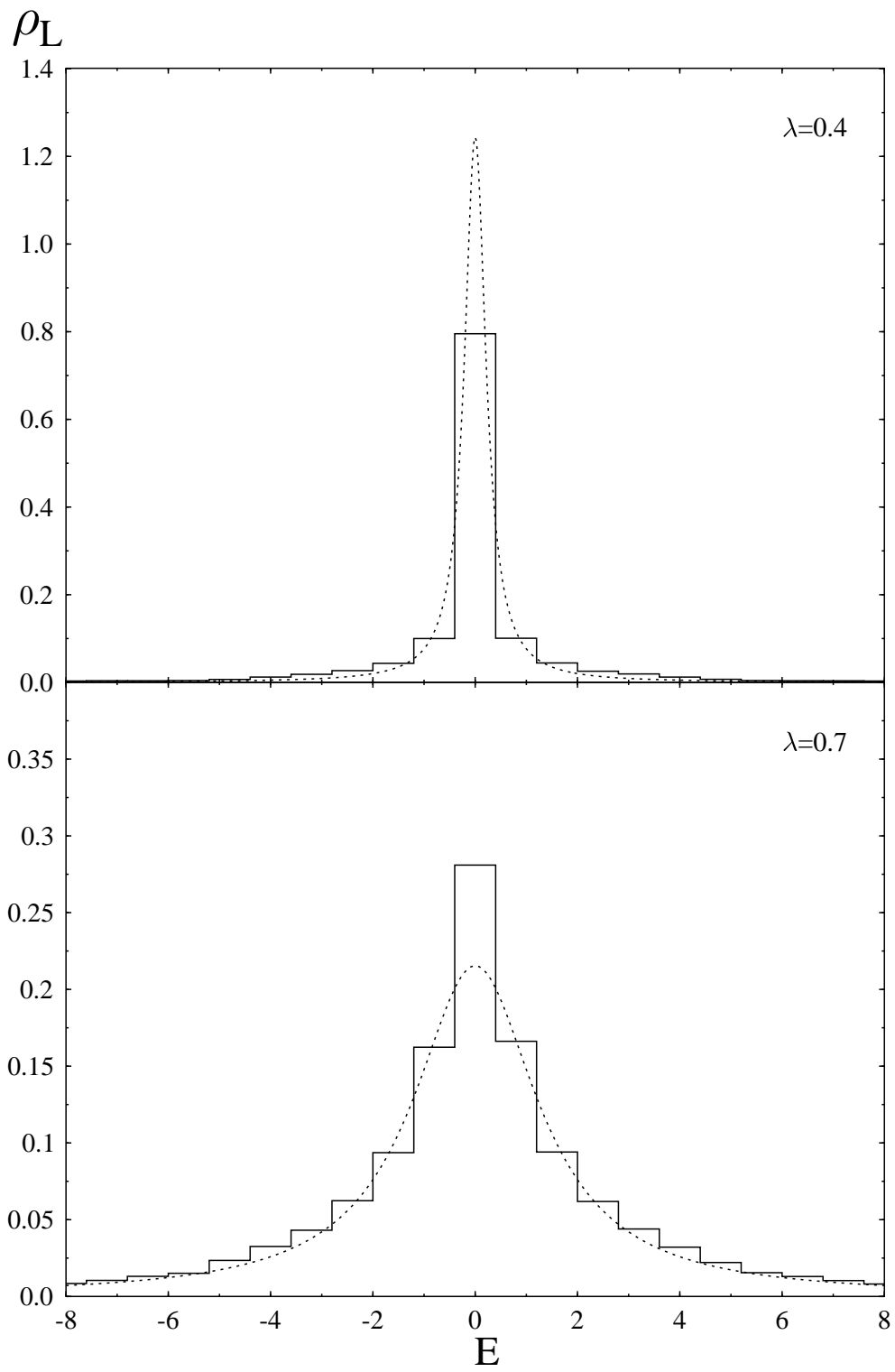


Fig.11



ρ_L^{rs} 





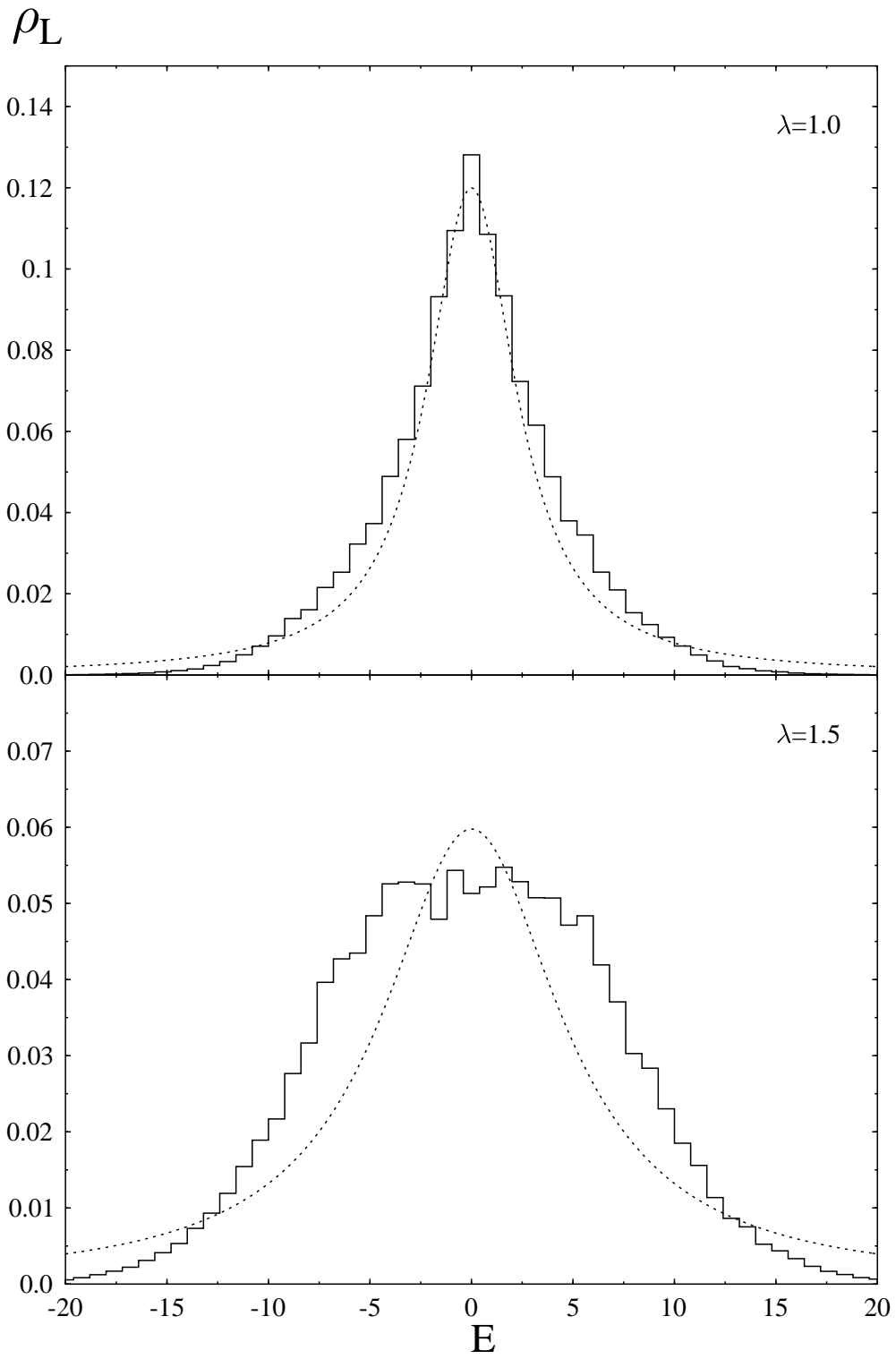


Fig.16

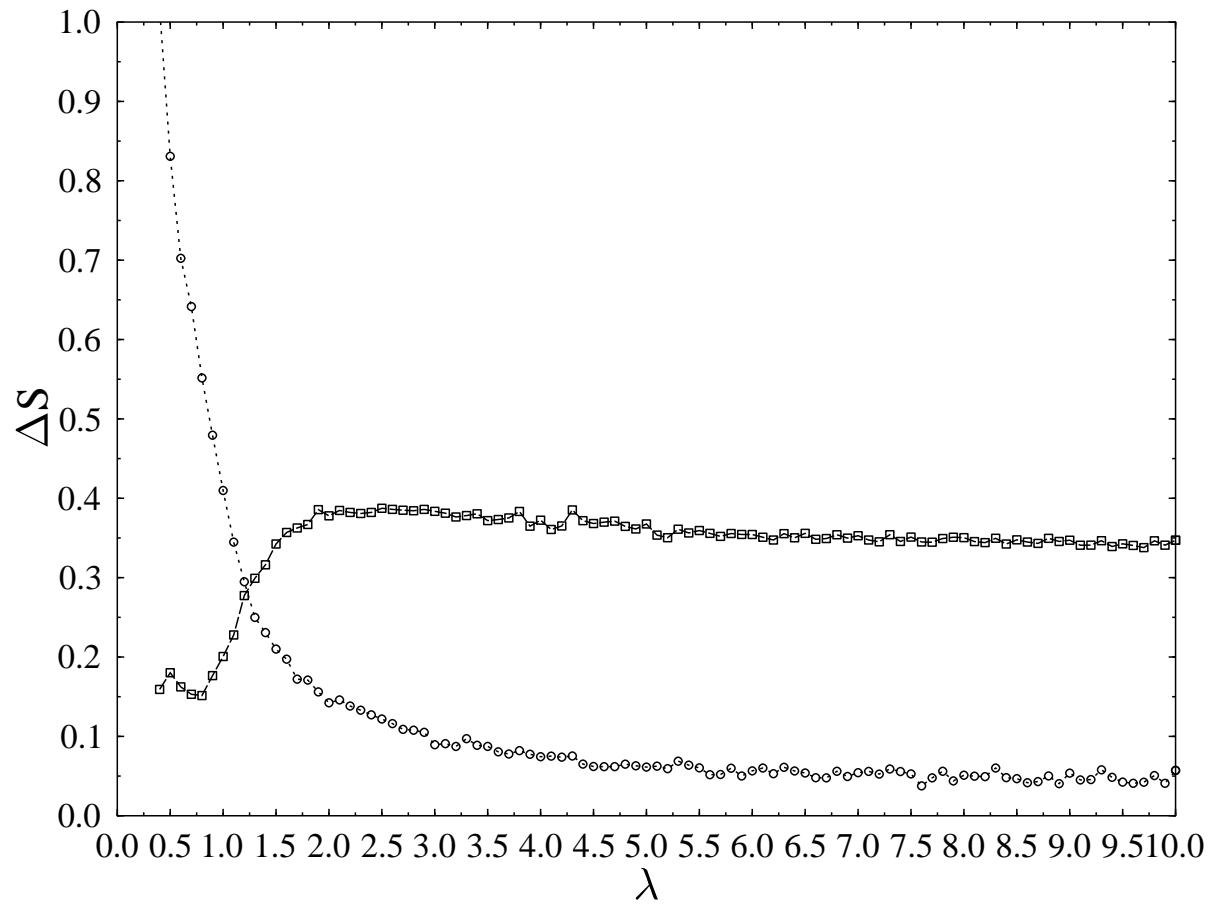


Fig.17

